This is a reproduction of a library book that was digitized by Google as part of an ongoing effort to preserve the information in books and make it universally accessible.

Google books

https://books.google.com

UNCLASSIFIED

Y 3.At7
22/US NRDL-TR-139

S

Copy No. 229

A FALLOUT FORECASTING TECHNIQUE WITH RESULTS OBTAINED AT THE ENIWETOK PROVING GROUND

Research and Development Technical Report USNRDL-TR-139

NS 081-001
U.S. Army

3 April 1957

by

E.A. Schuert

U.S. NAVAL RADIOLOGICAL DEFENSE LABORATORY

SAN FRANCISCO 24 · CALIFORNIA

DOCUMENTS
OCT 23 1957
U. OF W. LIBRARY

UNCLASSIFIED
UNIVERSITY OF MICHIGAN
3 9015 09521 8262
Digitized by Google

Reproduction of this document in any form by other than activities of the Department of Defense is not authorized unless specifically approved by the Secretary of the Navy or the Chief of Naval Operations as appropriate.

12ND P1923
NAVY-DPPO-12ND-MI

Digitized by Google

UNCLASSIFIED

A FALLOUT FORECASTING TECHNIQUE WITH RESULTS OBTAINED AT THE ENIWETOK PROVING GROUND

Research and Development Technical Report USNRDL-TR-139

NS 081-001
U.S. Army

3 April 1957

by

E.A. Schuert

Physics

Technical Objective
AW-7

Radiological Capabilities Branch
T. Triffet, Head

Chemical Technology Division
E. R. Tompkins, Head

Scientific Director
P.C. Tompkins

Commanding Officer and Director
Captain Richard S. Mandelkorn, USN

U.S. NAVAL RADIOLOGICAL DEFENSE LABORATORY
San Francisco 24, California

UNCLASSIFIED

Digitized by Google

ABSTRACT

A generalized fallout forecasting technique is presented with detailed computations of input parameters which were used at the Eniwetok Proving Ground.

Results obtained at a recent weapons test are briefly discussed by comparison of forecast fallout with preliminary measured data.

Digitized by Google

SUMMARY

The Problem

A fallout forecasting technique is needed to qualitatively describe the fallout hazard resulting from nuclear detonations. This technique should have such flexibility that its employment is valid for field use.

Findings

A summary of the latest experimental and theoretical considerations has resulted in the development of a technique whose complexity is dependent on the required accuracy of the results desired. Such a technique has been satisfactorily tested at the Eniwetok Proving Grounds for land surface and water surface bursts.

Digitized by Google

Digitized by Google

ADMINISTRATIVE INFORMATION

This work was done under Bureau of Ships Project No. NS 081-001, Subtask 1, Technical Objective AW-7, as described in U.S. Naval Radiological Defense Laboratory Annual Progress Report (DD Form 613) to the Bureau of Ships, July 1956.

The fallout studies were made at Operation REDWING, Project 2.6.3, as described in DD Form 613, NS 088-001, Subtask 4B, Encl (1) to CO USNRDL Secr ltr 3-905-335 Ser 0014173 of 16 March 1956.

The work also is part of the technical program for the Department of the Army established between Department of the Army, Office, Chief of Research and Development, and Bureau of Ships (Joint Agreement, 23 November 1955).

Digitized by Google

CONTENTS

Digitized by Google

ILLUSTRATIONS

Digitized by Google

Digitized by Google

TABLES

Digitized by Google

Digitized by Google

1 INTRODUCTION

Fallout research continues to seek a theoretical working model that will describe in detail the mechanism of fallout. Aside from this long-range problem, consideration must be given to making available a working tool that will meet the needs of the military for solving fallout problems in the field. Such consideration requires a simplified rapid system capable of producing qualitative if not quantitative results.

Within a program studying fallout at a recent weapons test operation there was a fallout forecasting assignment that had many aspects of the practical field problem yet, at the same time, required quantitative results for use in reducing other data. This program needed positioning data such that three ships could be located properly in the fallout to obtain data on its parameters. Also, aerial and oceanographic survey projects required knowledge of the fallout to instigate their navigational procedures properly.

To meet these requirements a technique for rapid fallout forecasting was developed which not only satisfied the needs of the fallout program but also was accurate enough to allow comparison between the meteorological aspects of model work and the results obtained from surface measurements. This technique was restricted to describing quantitatively the perimeter of the fallout, the axis of the "hot line," and to determining the time of arrival of fallout throughout the pattern. No attempt was made to quantitate the expected levels of gamma activity or to develop radiation contour lines.

At this operation the Task Force employed a fallout prediction unit for determining the safe time to detonate the test devices. Although many of their techniques for forecasting were similar to those described in this report, their problem was of a different nature than that of the fallout program. Several of their methods were unique in that portable analog computers were tested as field instruments. These computers permitted consideration of many complex parameters. One, in particular, obtained essentially an instantaneous solution to the problem once the meteorological data were available.

Digitized by Google

The fallout program and the Task Force prediction unit functioned independently. It was not feasible for the two to employ the same technique because the post shot variability of the winds aloft were especially critical in ship location problems of the fallout program. This problem will be discussed in detail later.

1.1 Objective

This report describes a technique for forecasting fallout employed at a recent weapons test operation. The results obtained in the field are discussed as examples of the reliability of the techniques. Although the technique was designed for analysis of land surface detonations where the fallout is particulate, its application to water surface detonations is considered.

2 FORECASTING TECHNIQUE

The forecasting technique uses many ideas from fallout model work. Several simplifications, as well as a plotting device, have been developed to the end that the time involved has been reduced greatly without sacrificing accuracy. In general, an initial source of activity is defined describing the "stabilized" nuclear cloud by appropriate spatial and size distributions of radioactive particles. These particles are tracked to the earth's surface by considering their falling speeds and effects of the winds existing aloft.

2.1 Basic Considerations

In some cases the input parameters for the forecasting technique were obtained from weapons test measurements. In others, where data were lacking, the parameters were derived from theory.

2.1.1 Source Model

The optical or visible dimensions of the initial cloud from a nuclear detonation have been documented in past weapons tests. Available data describe such parameters as height to base of mushroom, height to top of mushroom, and mushroom diameter as functions of time. Vertical rise stabilizes in approximately 6 min post detonation. This time is independent of yield however, the expansion of the mushroom diameter, particularly for the megaton devices, continues for perhaps 30 min. Available diameter measurements have not been made in excess

Digitized by Google

of H+10 min, however fairly reliable data are known for the optical cloud dimensions as functions of yield to H+10 min. The ultimate cloud diameter can be extrapolated from low yield curves and some qualitative data. Figures 1 and 2 present values of the cloud dimensions from past tests. The source model was assumed cylindrical having, for a given yield, these dimensions. Its stem diameter was taken as 10 percent of mushroom diameter.

2.1.2 Activity Distribution in Source Model

The greater part of the activity was assumed to be concentrated in the lower third of the mushroom. The lower two-thirds of the stem was ignored; the remainder of the stem and upper two-thirds of the cloud were weighted lightly. This description (Fig. 3) of the activity distribution within the cloud appeared most reasonable in the light of available data and logical theoretical considerations. The activity was concentrated nearer the axis of symmetry of the cloud than at its outer edges.

2.1.3 Particle Size Distribution in Source Model

All particle sizes were assumed at all elevations within the cloud except the lower two-thirds of the stem. However, to obtain agreement with past fallout measurements and with the optical diameter of the mushroom, it was necessary to fractionate the particle size distribution radially within the cloud. Otherwise the computed fallout area about ground zero would be too large. The fractionation was specified as follows: particles of 1000 microns in diameter and larger were restricted to the inner 10 percent of the mushroom radius or approximately the stem radius; those from 500 to 1000 microns in diameter were limited to the inner 50 percent of the cloud radius. Since the relation of activity to particle size is some direct function of the particle diameter,* this fractionation tends to concentrate the activity about the axis of symmetry of the cloud.

2.1.4 Particle Falling Speeds or Settling Rates

Computations of the terminal velocities of the particles were based on aerodynamic considerations for a still atmosphere having temperature and density distributions typical of the Marshall Islands atmosphere in the spring months.

Experimental data from past tests at Eniwetok Atoll indicated that the particles were irregular in shape and had a mean density of 2.36 g/cu cm.

---

* Unpublished data from a recent weapons test.

Digitized by Google

It can be shown that particles falling at their terminal speed experience three types of flow in a fluid: streamline or laminar flow where viscous forces predominate ($10^{-4} \leq R_e \leq 2.0$); intermediate flow where inertia forces predominate ($2 \leq R_e \leq 500$); and turbulent flow where inertia forces predominate ($500 \leq R_e \leq 10^5$). Below a Reynolds number of 10^{-4} certain corrections must be applied to the equations because the particle diameter approaches the mean free path of the fluid medium; the region above a Reynolds number of 10^5 is important only in ballistics. These limiting cases will not be discussed here.

The parameters actively affecting a particle's falling speed are: its weight; its drag coefficient; its density; as well as the fluid density and fluid viscosity.

Most empirical equations developed in past experimental work have been for spheres dropped in various liquids. Some work has been done on irregular-shaped particles and some done in wind tunnels. The equations[1] used to determine the falling rates for particles in a fluid medium follow.

<u>For streamline motion, $10^{-4} \leq R_e \leq 2.0$</u>

$$V_s = K_s \left(\frac{\rho - \rho_o}{\rho_o} \right) (d^2) \left(\frac{\mu}{\rho_o} \right)^{-1} \qquad (1)^*$$

where

V_s = terminal velocity in cm/sec

ρ = particle density in gm/cm³

ρ_o = fluid density in gm/cm³

d = particle diameter in cm

u = absolute viscosity of fluid in poises

K_s = constant incorporating gravity

= 54.5 for spheres

= 36.0 for irregular-shaped particles.

---

* This equation was taken from Ref 1. However, certain constants have been re-evaluated.

Digitized by Google

The limiting diameter to which Eq (1) holds is:

$$d' = \left(\frac{36\mu^2}{g\rho_o(\rho-\rho_o)}\right)^{1/3}$$ for spheres and

$$d' = \left(\frac{54.4\mu^2}{g\rho_o(\rho-\rho_o)}\right)^{1/3}$$ for irregular-shaped particles.

For Intermediate motion, $2.0 \leq R_e \leq 500$

$$V_I = K_I \left(\frac{\rho-\rho_o}{\rho_o}\right)^{2/3} \left(\frac{\mu}{\rho_o}\right)^{-1/3} d_o \qquad (2)^*$$

where

$d_o = d - \xi d'$

$\xi = 0.4$ for spheres

$\xi = 0.279$ for irregular shapes

d' = limiting diameter to which streamline motion applies

$K_I = 30.0$ for spheres

$= 19.0$ for irregular-shaped particles.

The limiting diameter to which the Eq (2) holds is:

$$d'' = 43.5\left(\frac{\mu^2}{g\rho_o(\rho-\rho_o)}\right)^{1/3}$$ for spheres

$$d'' = 51\left(\frac{\mu^2}{g\rho_o(\rho-\rho_o)}\right)^{1/3}$$ for irregular-shaped particles.

For turbulent motion, $500 \leq R_e \leq 10^5$

$$V_T = K_T\left[\left(\frac{\rho-\rho_o}{\rho}\right)d\right]^{1/2} \qquad (3)^*$$

$K_T = 54.6$ for spheres

$= 50.0$ for irregular-shaped particles.

---

* These equations were taken from Ref 1. However, certain constants have been re-evaluated.

Digitized by Google

The average falling rate for a group of irregular-shaped particles of a given size will be given by the equations. However, individual particles of the group may deviate from this average.

2.1.5 Marshall Islands Atmosphere

Marshall Islands atmospheric conditions determined the values for the density and viscosity parameters used in computing particle falling rates. Available data on the temperature, pressure, density, and viscosity as functions of altitude for the atmosphere common to the Marshall Island area in the spring months follow.

It was not possible to use a "standard atmosphere" in this problem because such use introduced a large error in the particle falling rate at high altitudes. This error originates primarily because an isothermal layer is assumed above the tropopause in the standard atmosphere — an unrealistic assumption.

Temperature Distribution. From the weather data published by Task Force Weather Central at Operation CASTLE, four published radiosonde runs obtained temperature measurements to high altitides:

1 March 1954 0600 M Bikini

27 March 1954 0600 M Bikini

7 April 1954 0620 M Bikini

26 April 1954 0610 M Bikini

No data were available above 67,000 ft. Fortunately two of these runs penetrated the tropopause which was located at approximately 55,000 ft. To extend the measured data beyond 67,000 ft, climatological averages[2] for latitude 12°N were employed. Agreement with measured data was satisfactory except for the range from 50,000 to 65,000 ft where the climatological data indicated a well-defined isothermal layer. The most significant finding from the measured data was the complete lack of an isothermal layer above the tropopause. Instead, a distinct and rapid inversion was observed which, when extrapolated as a straight line, agreed with the climatological data above 70,000 ft. Since the atmosphere was to be defined to 120,000 ft, further extrapolation was necessary. Temperature data available at these higher altitudes were taken by rockets[3] over White Sands, New Mexico. A plot of three points from the rocket data justified to some extent a continued extrapolation of the curve to 120,000 ft.

Digitized by Google

Therefore the profile of the vertical temperature gradient (Fig. 4) was based on measured data to 67,000 ft and extrapolated to 120,000 ft on the basis of supporting climatological data and temperature measurements made at high altitudes with rockets.

Pressure Distribution. Published high altitude measurements of the pressure distribution were obtained on two occasions at Operation CASTLE. These measurements,* made at Bikini on 7 April 1954 and on 26 April 1954, were not taken above 65,000 ft. Above this altitude the pressure was extrapolated as a straight line on semi-log paper to 120,000 ft. Agreement with published rocket data from White Sands, New Mexico was good to 90,000 ft (Fig. 5).

Density Distribution. The density distribution of the atmosphere (Fig. 6) was calculated from the perfect gas law using the above pressure and temperature distributions,

$$\rho = \frac{P}{RT}$$

where the gas constant was taken for dry air. The assumption of no moisture in the mixture introduces an error of several percent in the lower layers of the atmosphere where the relative humidity is high. However, this assumption can be safely neglected. Also, the latest theories on the composition of the atmosphere indicate it to be constant to altitudes above 150,000 ft which justified the assumption of a non-varying gas constant.

Viscosity Distribution. The variation of absolute viscosity with altitude was computed from the observed temperature distribution using Sutherland's formula,[4]

$$\mu = \mu_o \left(\frac{T_o + 114}{T + 114}\right) \left(\frac{T}{T_o}\right)^{3/2}$$

$$\mu = 0.01709 \left(\frac{387.17}{t_i + 114}\right)\left(\frac{t_i}{273.17}\right)^{3/2}$$

where t_i = temperature in degrees Kelvin and μ is viscosity in centipoises. These data are plotted in Fig. 7.

* Hq. T.U.-13 Operation Memo No. 14, 30 April 1954.

Digitized by Google

The data on pressure, temperature, density, and viscosity in 1000-ft intervals to 120,000 ft are summarized in Table 1.*

2.1.6 Terminal Velocity Computations

The average falling speed through 5000-ft layers was computed for four particle sizes over an altitude range from 0 to 120,000 ft. In these computations all in-flight transition of the particles from streamline to intermediate flow had to be considered through use of the plot shown in Fig. 8.

Four particle sizes (75, 100, 200, and 350 μ diameter) were employed since there was evidence from past tests that the 75-μ particle defined the limiting distance of fallout of interest and the larger sizes best described the pattern within this limit. Table 2 presents the falling speeds computed for the four sizes. Tables 3, 4, 5, and 6 display the cumulative time of fall from a given altitude for these particle diameters.

2.1.7 Meteorological Procedures

It is necessary to have available the best possible description of the winds aloft in order to determine the arrival points of particles of various sizes originating at various altitudes. Such data are usually availabel from the normal upper air soundings routinely taken by Weather Bureau and Military Meteorological stations. Although wind velocity as a function of height varies continuously, it can be described by an average speed and direction in discrete layers. Such averaging can best be obtained from the WBAN-20 Form where the original data are recorded. The technique employed in this report was to divide the atmosphere into layers 5000 ft thick and determine an average speed and direction for each layer. When the average falling speed of particles through these 5000-ft layers and the speed and direction of the wind are known, horizontal displacement can be computed. Thus, for each particle size a vector may be drawn for the average particle displacement in a particular 5000-ft layer. Addition of such vectors from all layers described the trajectory projection of a particle of given size. Similar plotting for all particle sizes originating at all elevations within the cloud source will map the fallout on the earth's surface.

This technique is valid for any atmosphere that has negligible vertical motion and is in a steady state condition with respect to the horizontal winds during the time needed for the slowest particle to fall from the highest altitude to the ground. Such an assumption is not realistic for situations arising from many of the megaton devices because 15 to 20 hr are necessary to establish the fallout area. Consequently, when computing particle trajectories, an attempt should be

* A great deal of excellent upper air data for the Marshall Islands was obtained at Operation REDWING in 1956. Reduction of these data will result in a much better description of the Marshall Islands atmosphere than has been previously available.

Digitized by Google

made to consider how the wind varies with time and how it varies with distance from ground zero; what effect vertical motions have on particle falling speeds and how they vary with space and time. Such considerations complicate computation of trajectories extremely. In most cases valid input data describing these variables are not available. This phase of the problem is discussed below.

2.2 Plotting Technique

The use of "particle-size" and "height" lines in mapping fallout is a standard technique employed by most analytical methods. This technique simply describes a grid (Fig. 9) on the earth's surface indicating where fallout particles of certain sizes will arrive and from what altitude they came. These parameters are the basic data for describing the fallout pattern.

Assuming steady state meteorological conditions without vertical motion or space variation of the winds, it is very easy to construct a grid describing arrival points on the earth's surface for particles of various sizes originating at different altitudes. This grid is constructed by ignoring the horizontal distribution of particles in the cloud model and by plotting those trajectories that originate along the line source describing the vertical axis of the cloud.

Plotting trajectories for each particle size at every starting elevation is the first step in determining the resultant fallout pattern; however, the drafting involved is tedious and time-consuming. This effort can be reduced greatly by plotting from the ground up, as is done in the construction of a wind hodograph. Such a plot is made by starting at ground zero and working up through the altitude increments to the desired elevation. Although this technique does not plot the trajectory of the particle, it does define the arrival points on the surface of the earth of particles starting at each altitude increment (Fig. 10). To plot these size-lines one must make the preliminary computations of particle-falling times through each altitude increment to obtain the displacement for various wind velocities as described earlier in the Section on Terminal Velocity Computations (p 8).

A plotting device (Fig. 11), described elsewhere,[5] facilitates the computations required for the size-lines of the fallout pattern. Such devices were constructed for four particle sizes: 75, 100, 200, and 350 μ in diameter. With these plotters, trajectories or size-lines can be plotted from any elevation up to 120,000 ft for the four particle sizes. The plotters automatically account for the variable particle falling speed. They also eliminate the need for drafting equipment. After establishing the particle arrival points by either the use of size-lines or trajectories, height lines can be constructed. These lines, joining

Digitized by Google

surface zero with the arrival points of all particles from the same elevation, are most descriptive for they define the path along which all particle sizes will deposit from that originating altitude.

The height lines describing the fallout from the lower portion of the mushroom immediately establish the "hot line." The "hot line" is best defined as that portion of the fallout area wherein the highest levels of activity are found relative to the adjacent areas. Under most meteorological conditions this area is described by a line from surface zero that coincides with the height lines from the altitude layers that include the base of the mushroom; for the source model was so defined to concentrate the activity in this volume.

Since the plotted grid of size-lines and height-lines was based on a line source of activity, each particle point must be expanded to the appropriate cloud or stem diameter from which it originated. This expansion, after taking into consideration the radial particle size fractionation in the source model, defines the perimeter of the area. One then has a map indicating the fallout area and the path of expected highest activity.

Curves of time of arrival of fallout through the pattern are established by simply assigning the appropriate value of falling time to each expanded circle about the arrival points and by constructing from this network of values iso-time contours that indicate the earliest time at which fallout will arrive at a given distance from the shot point. Similarly, the determination of the time of cessation of fallout at any location may be plotted. However, one is faced with the question of how to define cessation. Very small particles that do not contribute significantly to the radiation field continue to arrive for days after time zero. Consequently, a plot which describes time-to-peak activity seems more meaningful. During the field operation time-to-peak activity was defined as the time of arrival of fallout particles originating in the lower third of the mushroom.*

This method determines the fallout plot under conditions that do not involve several important meteorological variables. In this sense it is most valid for a fallout of short duration and over a relatively small area, for example, a 1-KT surface detonation. Megaton devices and large KT yields deposit primary fallout over long periods and to great distances. To map such extensive deposition of fallout necessitates inclusion of complex meteorological variables and consideration of the fact that clouds from these large detonations extend to great heights in the atmosphere.

---

* A recent study of available data indicates that the time-to-peak activity can be excellently defined as twice the time of arrival.

Digitized by Google

2.2.1 Time Variation of the Winds Aloft

In most of the observations made at the Eniwetok Proving Ground the winds aloft were not in a steady state. Significant changes in the winds aloft were observed in as short a period as 3 hr. This variability was probably due to the fact that proper firing conditions, which required winds that would deposit the fallout north of the proving ground, occurred only during an unstable synoptic situation of rather short duration. It was necessary to correct for this variation to keep track of the predicted fallout area, especially at great distances from surface zero where as much as 20 hr elapsed before deposition.

Since this variation could not be forecast, balloon runs were made every 3 hr from H+0 to H+24 and each particle trajectory employed the winds as they changed with time. The correct particle trajectories were approached by a method of successive approximations as follows: Tables 3 through 6 were computed for the four particle sizes and gave their cumulative times of fall such that starting at any elevation their altitude at any time after H-hr could be located. For example, the 75-μ particle originating at 70,000 ft entered the 40,000-ft layer in 7.18 hr and reached the surface in 19 hr. Since new upper air observations were obtained every 3 hr it was assumed that the balloon released at H+0 represented the winds aloft until H+3 hr and the balloon released at H+3 hr represented the winds until H+6 hr and so on. Therefore, as the particle settled to earth the appropriate winds aloft were applied to it.

The first step was to plot size-lines for the particles based on the H+0-hr winds. This established a fallout plot that assumed the winds would not change with time. When the H+3-hr winds became available a similar plot was made based on them. With the aid of Tables 3 through 6 the particles starting at various elevations were located in altitude at H+3-hr points. These H+3-hr points are marked at the proper altitude on each size line. The two size lines, H+0 and H+3,are then overlayed such that the H+3-hr points are coincident and the combined size-lines determined with the aid of a light-table. This is done by taking the upper portion of the H+0-hr size-line and the lower portion of the H+3-hr size-line. This first approximation then assumed that the H+3-hr winds will remain steady for the remainder of the particles flight. The process is repeated using the combined size-line and the new size-line for the next set of wind data until the particle reaches the surface. Therefore for each new wind observation a closer approximation of the corrected time variable plot is made until ultimately the plot is quantitative.

2.2.2 Space Variation

The preceding computations assumed that the winds aloft, as measured at the point of detonation, at a given time are the same throughout the area for that time. Since the fallout can deposit hundreds of miles

Digitized by Google

from surface zero, the ideal situation would be to take winds-aloft measurements throughout the volume traversed by the particles. Correction for space variation of the winds is then necessary, however in most cases not as significant as is time variation. Most weather networks are not refined enough to allow quantitative correction for these errors.

2.2.3 Vertical Motions

In applying particle falling speeds to the forecasting technique, it is assumed that the atmosphere has no vertical velocity. Computations made at the Eniwetok Proving Ground* to 50,000 ft indicated that large cellular vertical motions in the atmosphere sometimes attained speeds equal to and greater than the settling speed of a 75-μ particle. A time-space correction should be made for the falling speeds of the particles to compensate for this parameter. However, in the work at the test site it was not possible to include this effect in the fallout forecasts. Certain anomalies discussed below may be due to such an effect and post shot analysis is being conducted to see whether they are resolved when the vertical motions have been taken into account.

3 DISCUSSION OF FIELD TEST RESULTS

The forecasting technique described was employed by the fallout program at the Eniwetok Proving Ground to satisfy certain project requirements. One project had three ships equipped to collect fallout and their positions had to be determined for most efficient collection; another sampled the ocean for fallout; while another made an aerial survey of the contaminated area. The navigational schedules for these latter projects were based on the forecast fallout pattern. Operations were controlled through the Program Control Center aboard the Task Force Command Ship where the forecasts were prepared.

The meteorological data were received from the weather ship at Bikini atoll as well as from weather stations at Rongerik atoll and Eniwetok atoll. Furthermore, all forecasts made by the Task Force Weather Central at Eniwetok atoll were usually available aboard the command ship by facsimile through the ships Weather Station.

* Under the direction of CDR Daniel F. Rex, Joint Task Force Seven, Meteorological Center, Pearl Harbor, T.H.

Digitized by Google

Upper air measurements were made at Bikini, Rongerik, and Eniwetok atolls every 3 hr starting at H-24 hr and continuing until H+24 hr for any given detonation. The frequency of observations was usually increased during the period from H-6 to H-2 hr. The altitudes reached on the wind runs were remarkably high and gave perhaps the best set of winds-aloft measurements to date. The average termination altitude was approximately 90,000 ft with many runs over 100,000 ft. Such excellent coverage of the winds aloft was a major help in the fallout forecasting.

Fallout forecasts were made every 3 hr starting at H-24 hr, using the measured winds available at the time. This process was continued up to shot time and from then, on the technique of correcting for time variation, was employed every 3 hr until the fallout event was completed. It was not feasible to correct for space variation and vertical motions during this period because of the lack of time and data.

3.1 Fallout Plots

The fallout forecasts determined at the weapons test operation were based entirely on measured data and quantitatively considered time variation of the wind. No space variation corrections or computed values of vertical motions were employed in their construction.

The area of measured fallout from shot A is compared with the forecast fallout plot in Fig. 12. Figures 13, 14, and 15 are similar comparisons for shots B, C, and D. Although C and D were water surface shots, it is evident that the forecasting technique succeeded in representing the measured fallout area as well as it did for the land surface detonations, A and B.

The comparison is excellent for all shots except B and as yet the discrepancy between the forecast fallout area and that which was measured is unknown. There is some indication that consideration of vertical motions will have to be made for shot B during the time of fallout since computed vertical motions were significant in magnitude. Such analysis including space variation is being carried out at this time for all four detonations and the refined data will be published later.

4 SUMMARY

The fallout forecasting technique described in this report was successfully employed for both land surface and water surface detonations

Digitized by Google

at the Eniwetok Proving Ground. With known meteorological data such a technique will successfully quantify the area of fallout and indicate qualitatively the relative intensity of radiation.

Precise determination of the fallout area requires consideration of many complex meteorological parameters. However, from the above analysis a practical field tool can be developed that in most cases will satisfactorily define the area of interest.

Approved by:

E. R. Tompkins

E.R. TOMPKINS
Head, Chemical Technology Division

For the Scientific Director

Digitized by Google

REFERENCES

1. Dallavalle, J.M. Micromeritics, Pittman Publishing Corporation, New York, N.Y., 1948.

2. Brunt, D. Physical and Dynamical Meteorology, Cambridge University Press, London, 1941.

3. A Study of the Atmosphere Between 30,000 and 100,000 Feet (preliminary report), Chief of Naval Operations, Aerology Service Section, Washington D.C., September 1948.

4. Smithsonian Physical Tables, 1954.

5. Schuert, E.A. A Fallout Plotting Device, U.S. Naval Radiological Defense Laboratory Technical Report USNRDL-127, February 1957.

Digitized by Google

Digitized by Google

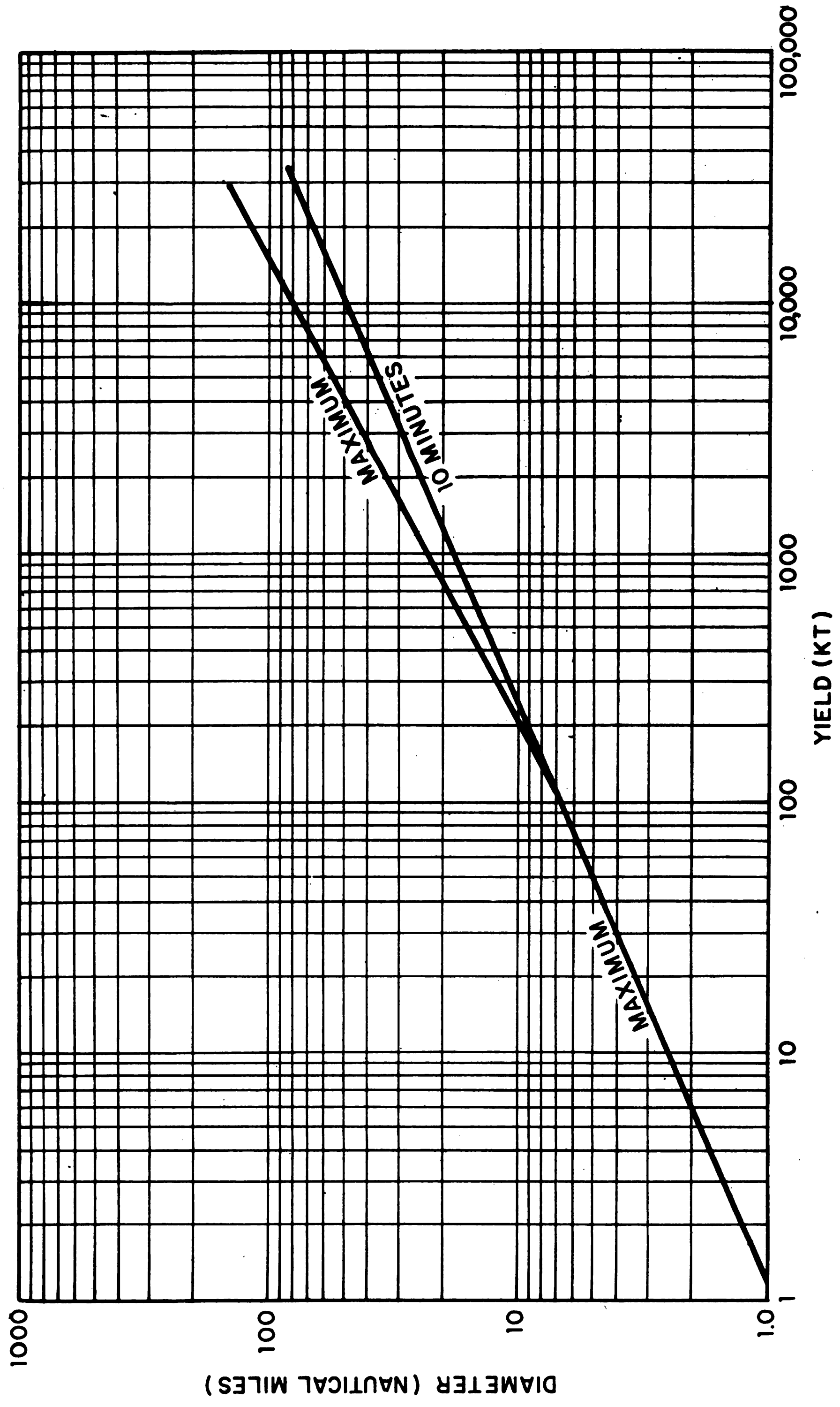

Fig. 1 Mushroom Diameter as a Function of Yield

Digitized by Google

Digitized by Google

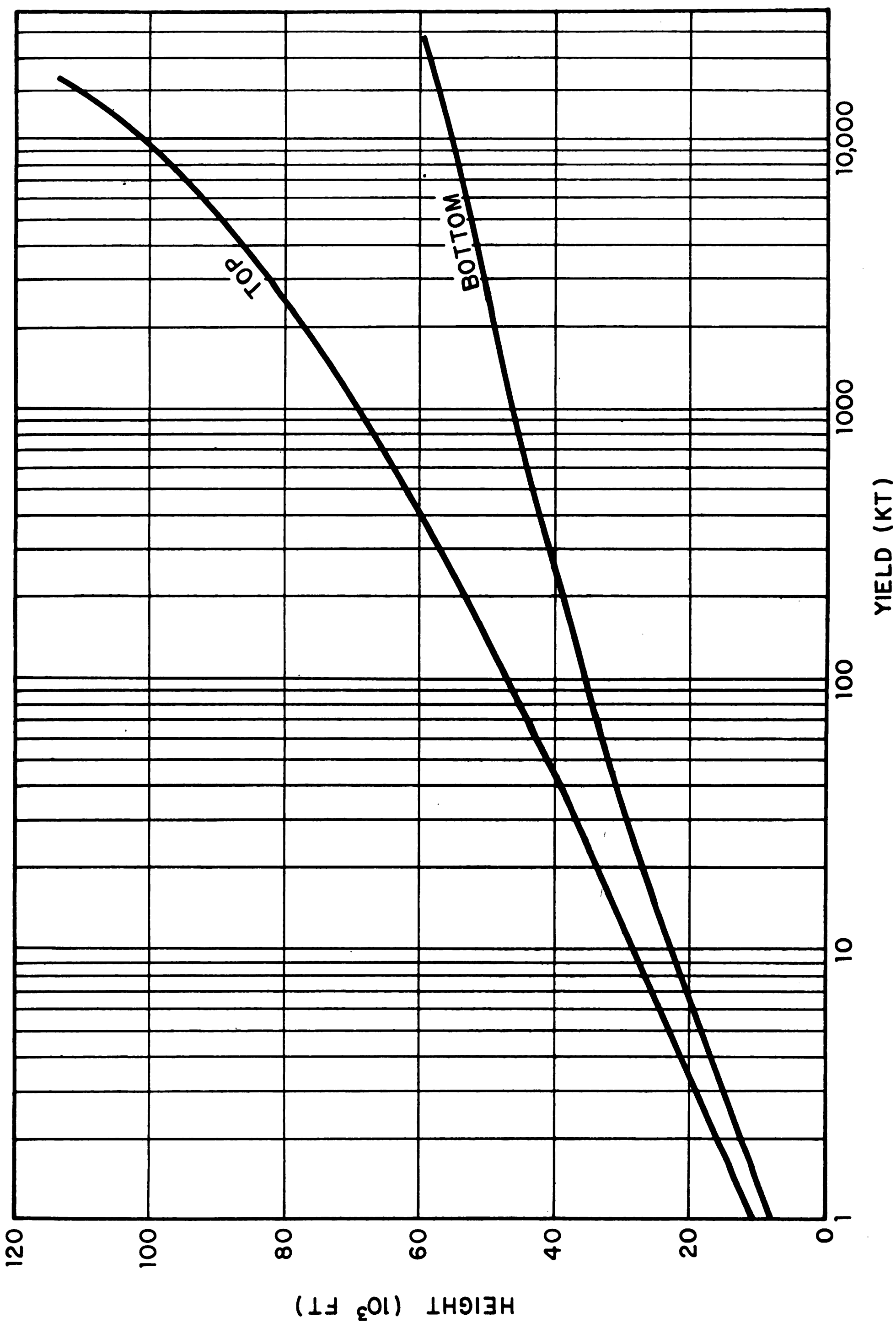

Fig. 2 Mushroom Height as a Function of Yield

Digitized by Google

Digitized by Google

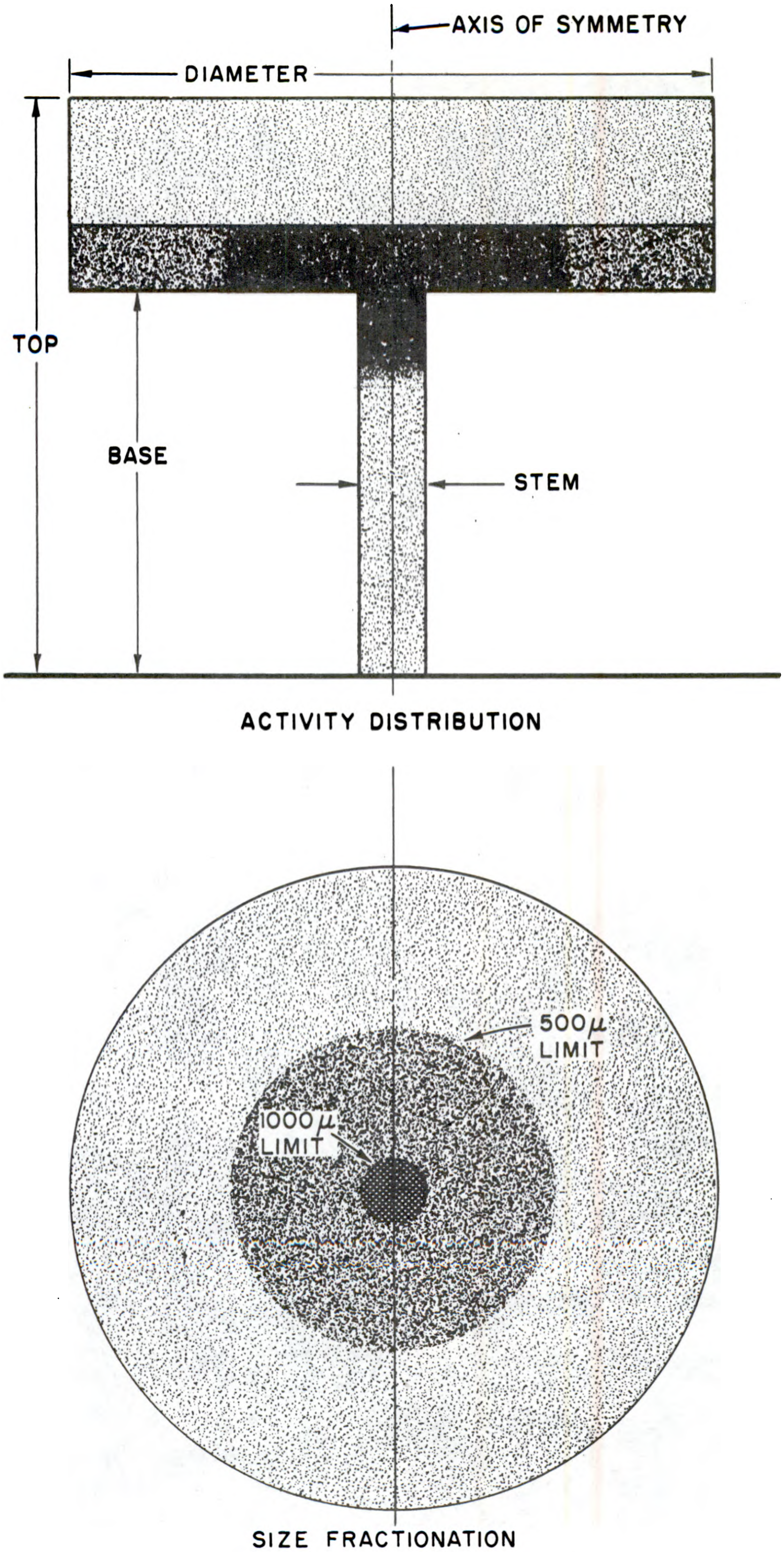

Fig. 3 Source Model

Digitized by Google

Digitized by Google

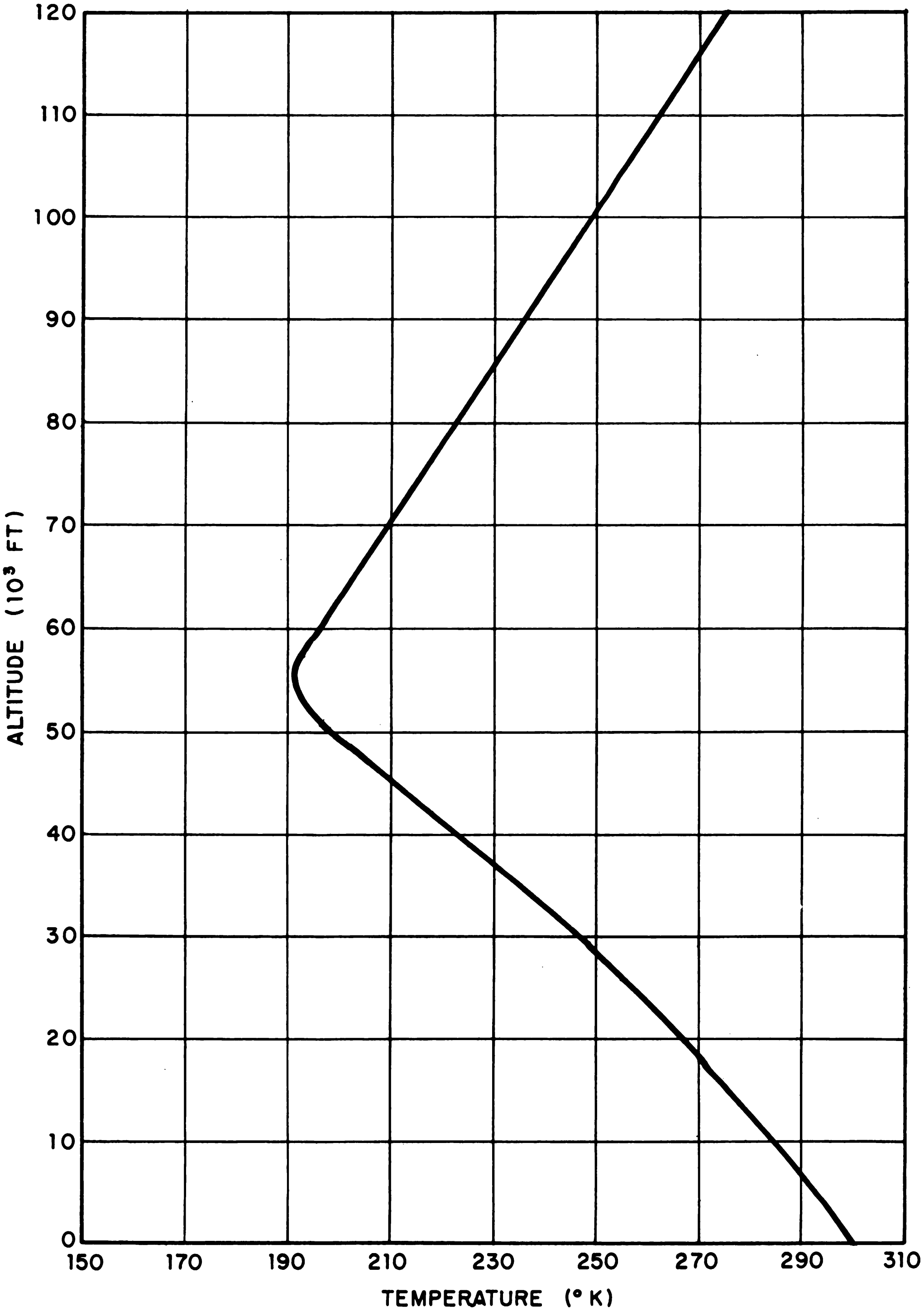

Fig. 4 Temperature as a Function of Altitude for a Marshall Islands Atmosphere

Digitized by Google

Digitized by Google

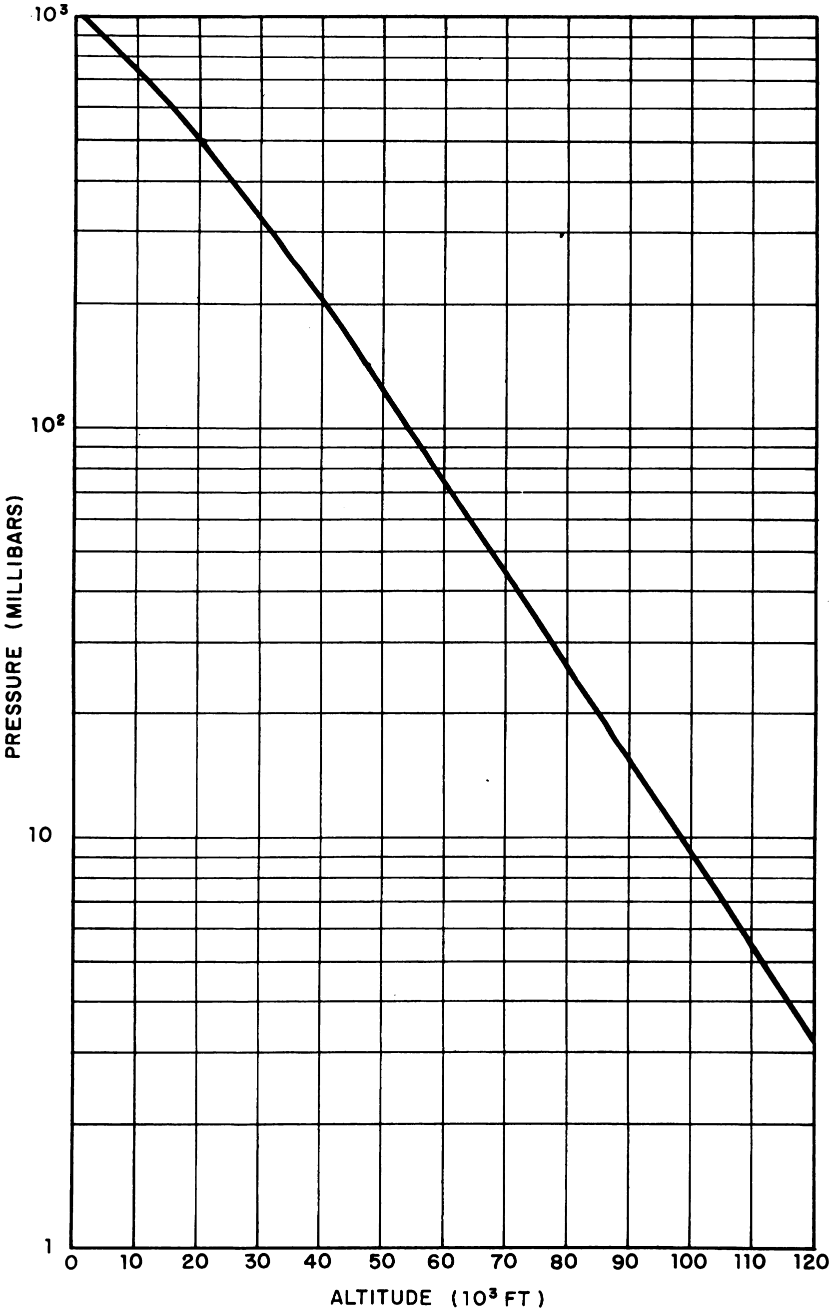

Fig. 5 Pressure as a Function of Altitude for a Marshall Islands Atmosphere

Digitized by Google

Digitized by Google

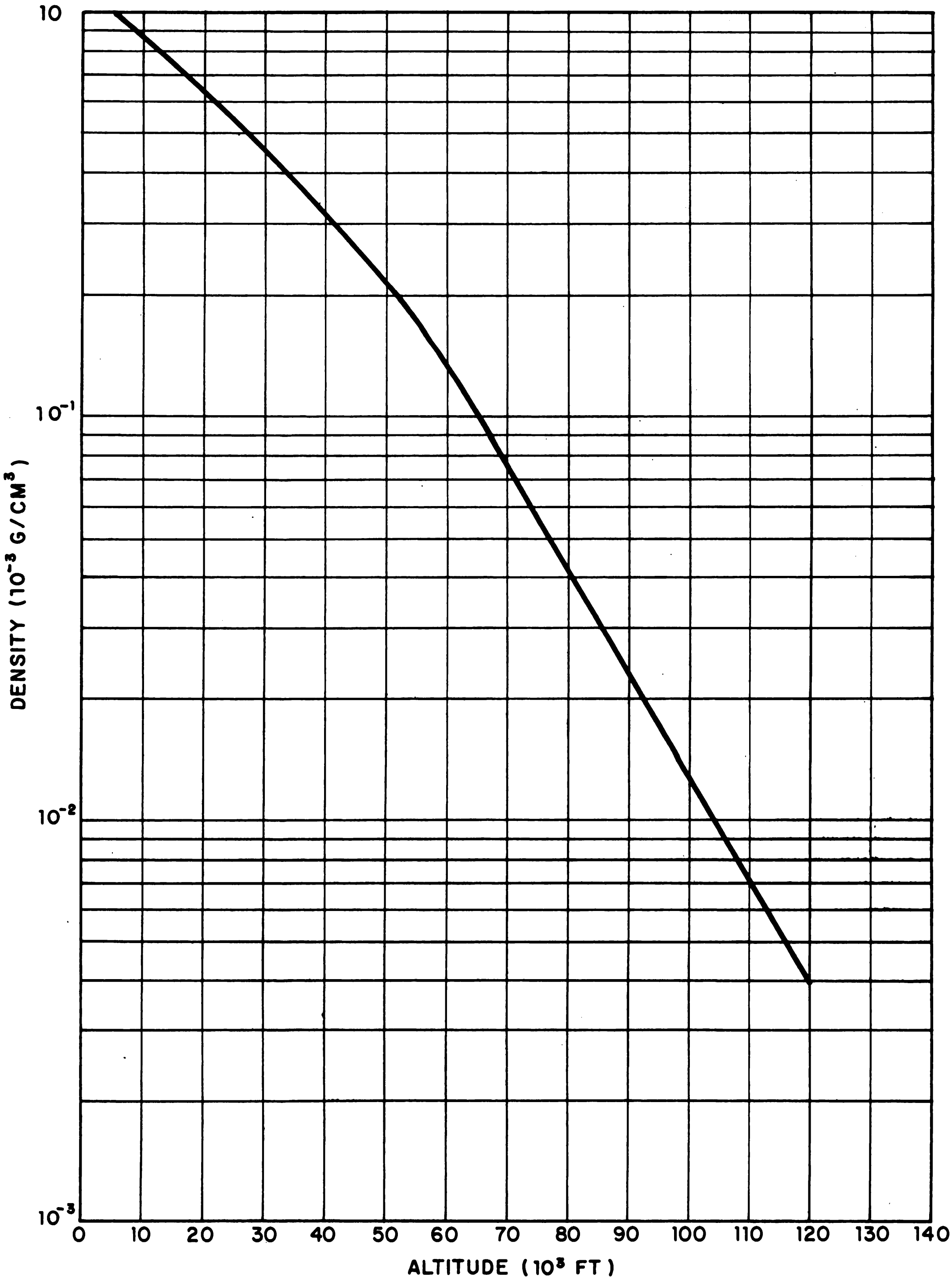

Fig. 6 Density as a Function of Altitude for a Marshall Islands Atmosphere

Digitized by Google

Digitized by Google

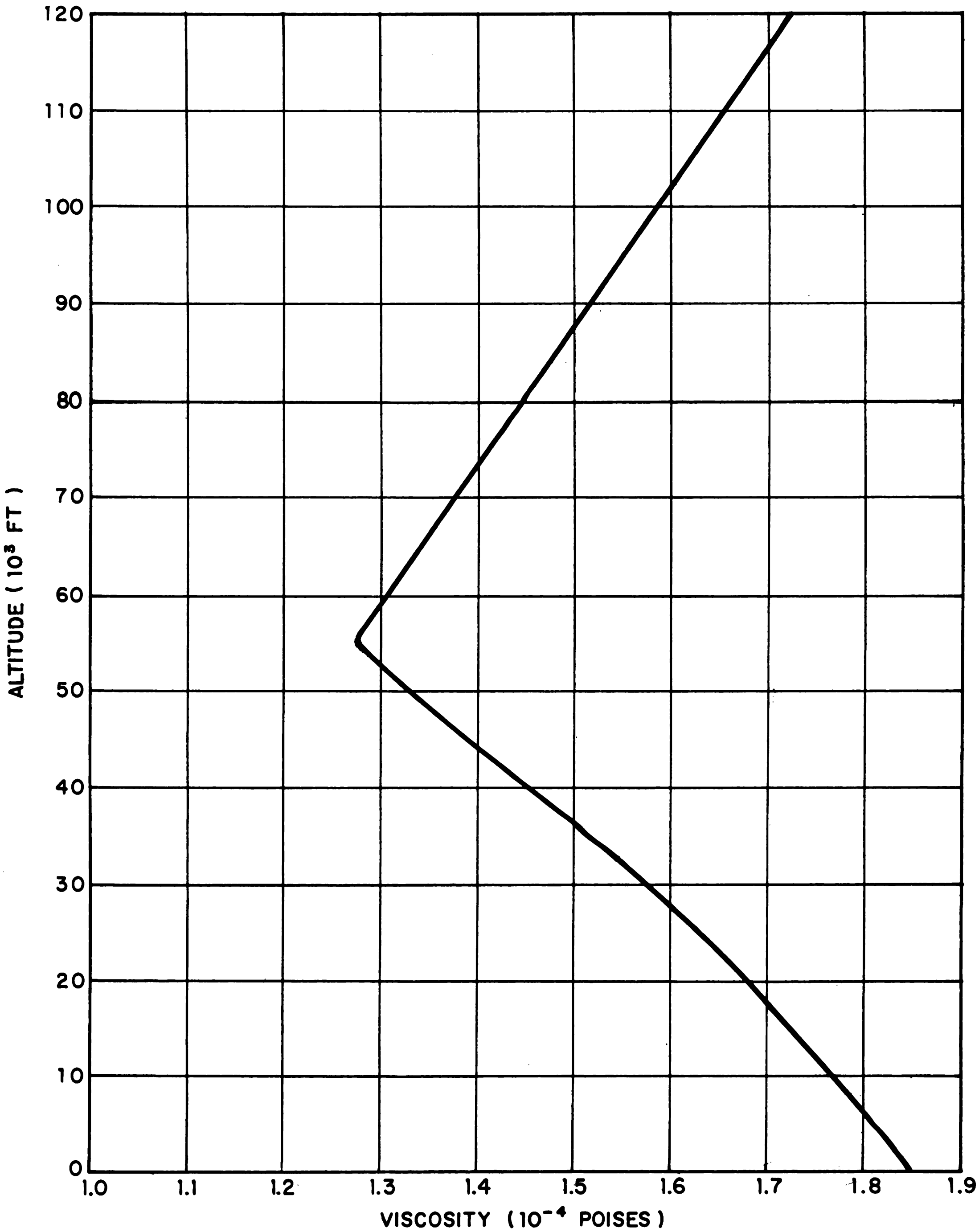

Fig. 7 Absolute Viscosity as a Function of Altitude for a Marshall Islands Atmosphere

Digitized by Google

Digitized by Google

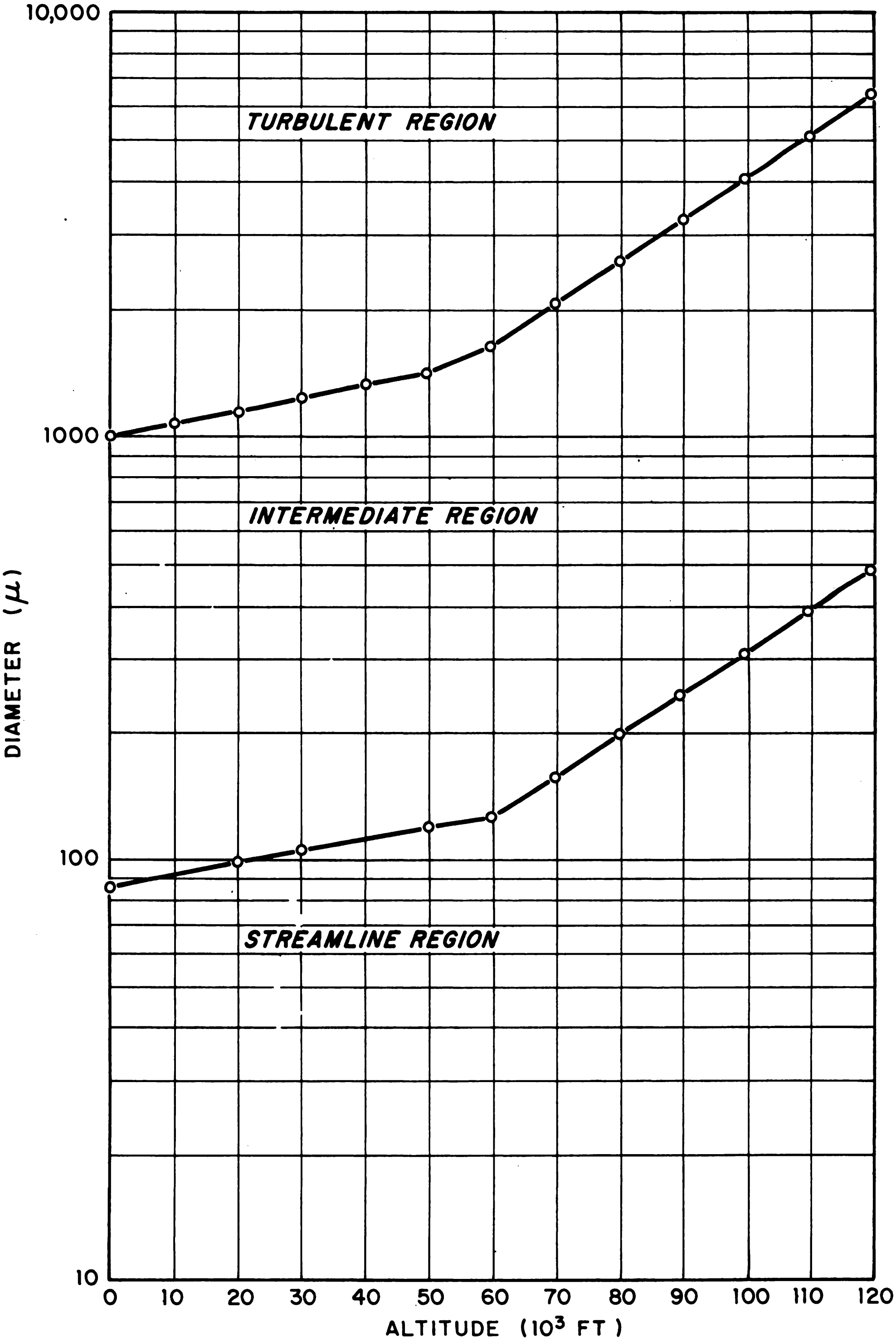

Fig. 8 Falling Speed Transition Zones for the Marshall Islands as a Function of Particle Size and Altitude

Digitized by Google

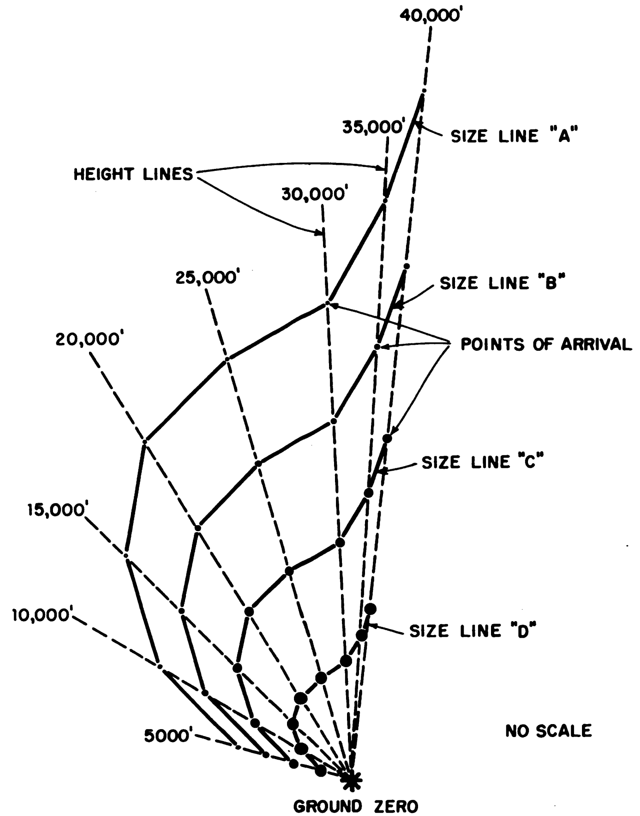

NOTE: Four particle sizes originating at altitudes up to 40,000 feet in a hypothetical wind field

Fig. 9 Basic Fallout Plot Showing Grid of Size Lines and Height Lines

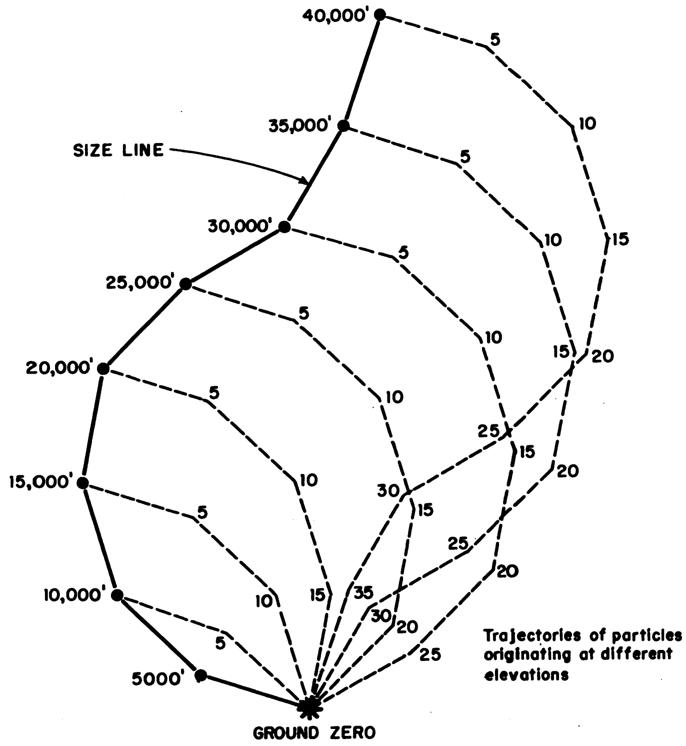

NOTE: Particles of the same size originating at altitudes up to 40,000 feet in a hypothetical wind field

NO SCALE

Fig. 10 Comparison of Plotting Techniques by Use of Trajectories or by Use of a Size Line

Digitized by Google

Digitized by Google

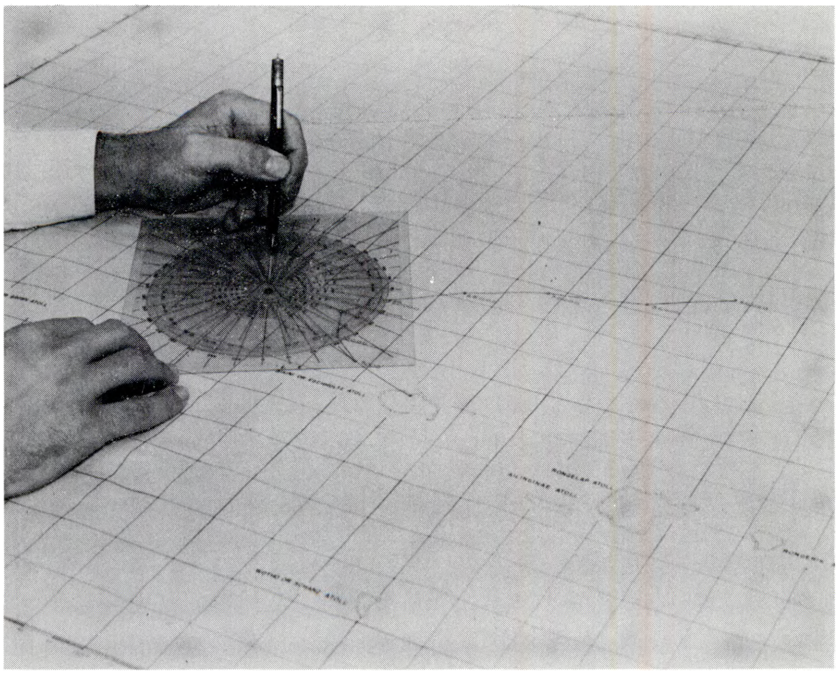

Fig. 11 Fallout Plotting Device.

Digitized by Google

Digitized by Google

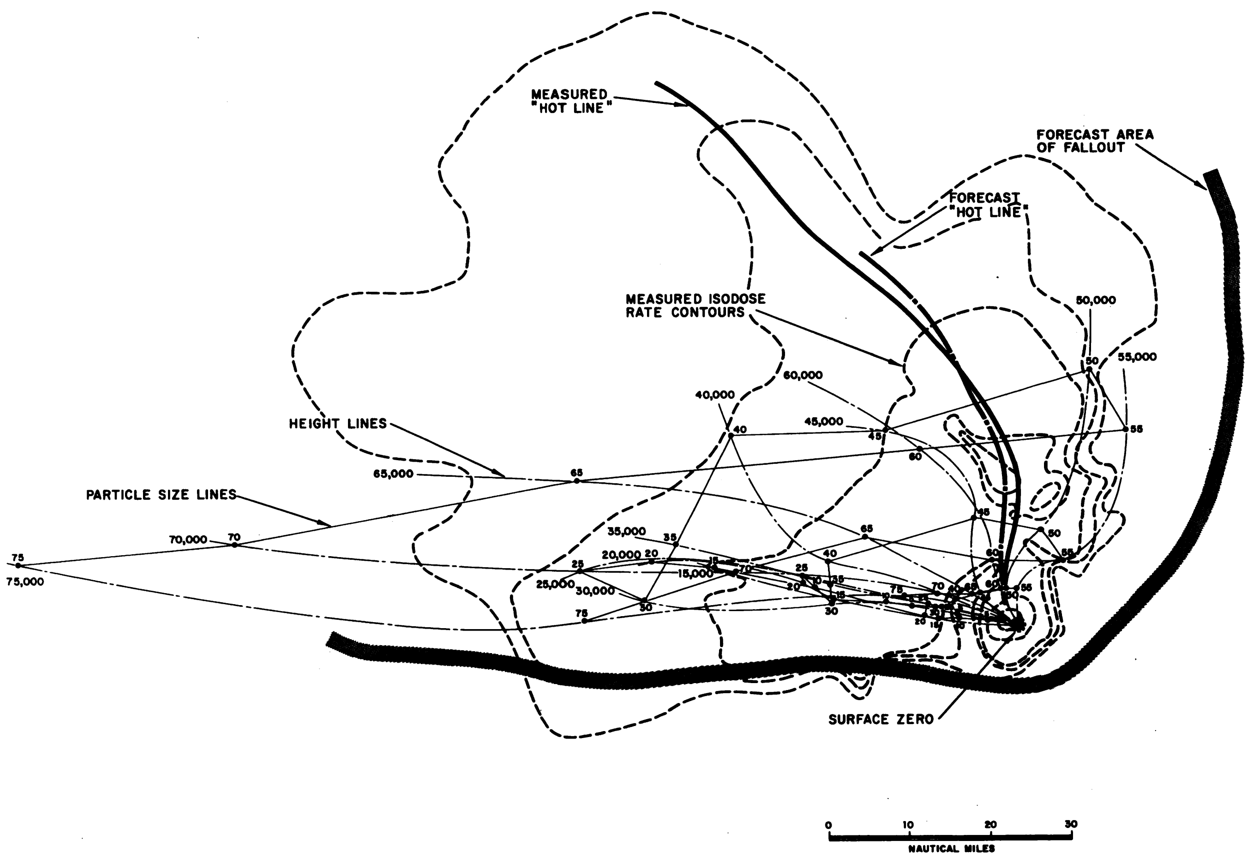

Fig. 12 Comparison of Fallout Forecast With Test Results - Shot A

Digitized by Google

Digitized by Google

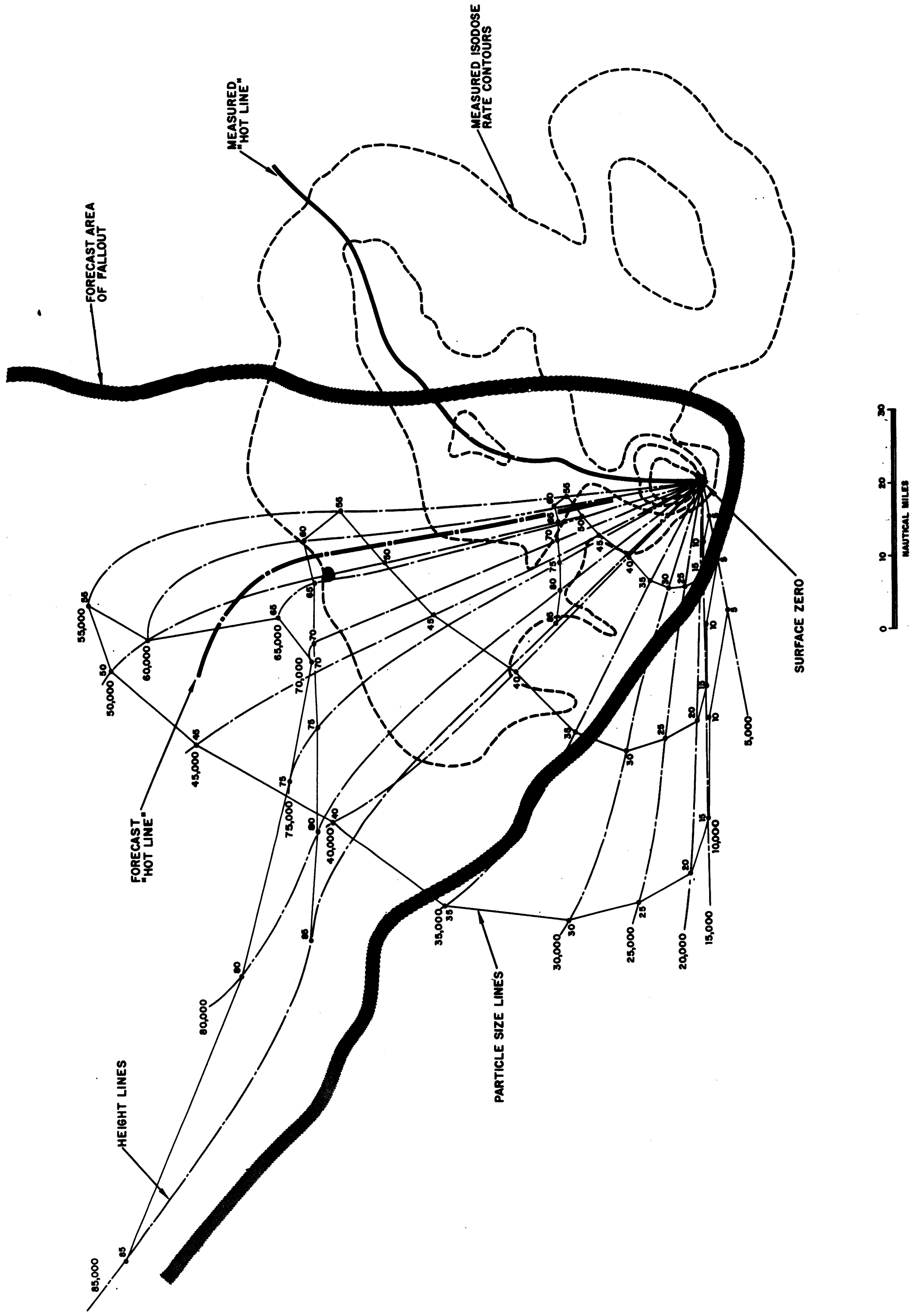

Fig. 13 Comparison of Fallout Forecast With Test Results - Shot B

Digitized by Google

Digitized by Google

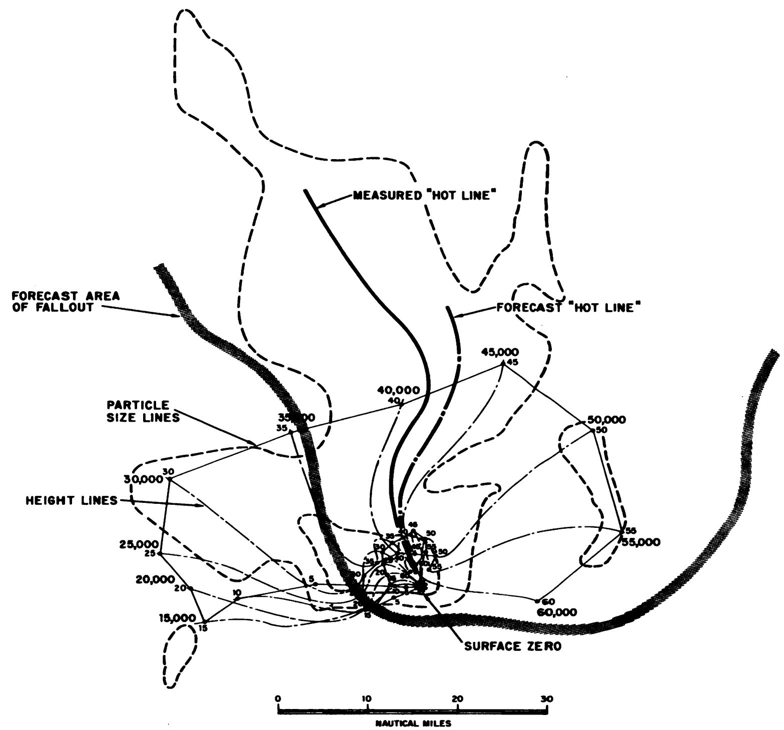

Fig. 14 Comparison of Fallout Forecast With Test Results - Shot C

Digitized by Google

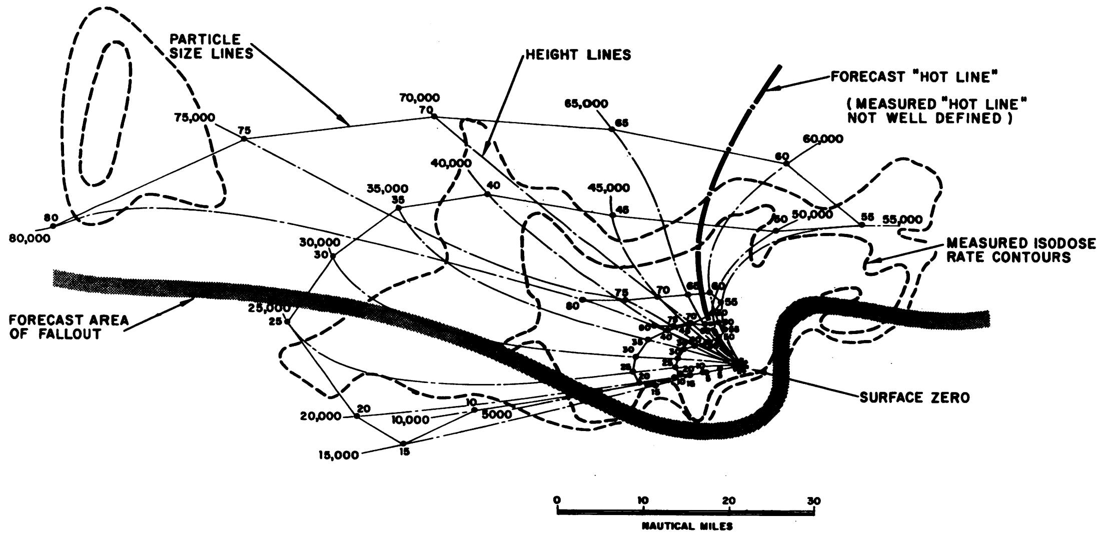

Fig. 15 Comparison of Fallout Forecast With Test Results - Shot D

Digitized by Google

TABLE 1

Temperature, Pressure, Density, and Viscosity of the Atmosphere Over the Marshall Islands During the Spring

Altitude (ft)	Temperature (°K)	Pressure (mb)	Density ($g/cm^3 \cdot 10^3$)	Viscosity ($poises \cdot 10^4$)
SFC	300	1006	1.17	1.84
1,000	299	980	1.13	1.83
2,000	297	950	1.10	1.825
3,000	296	930	1.06	1.815
4,000	295	900	1.03	1.810
5,000	293	870	1.0	1.805
6,000	292	850	0.97	1.795
7,000	290	820	0.94	1.785
8,000	289	800	0.91	1.780
9,000	288	770	0.88	1.770
10,000	285	740	0.86	1.765
11,000	284	720	0.83	1.755
12,000	282	690	0.80	1.745
13,000	280	660	0.78	1.740
14,000	278	640	0.76	1.730
15,000	276	620	0.73	1.720
16,000	274	590	0.71	1.715
17,000	273	570	0.69	1.705
18,000	271	550	0.67	1.695
19,000	269	530	0.65	1.685
20,000	267	500	0.63	1.675
21,000	265	480	0.61	1.665
22,000	263	460	0.59	1.655
23,000	261	440	0.57	1.645
24,000	259	420	0.55	1.635
25,000	257	410	0.53	1.625
26,000	255	390	0.52	1.615
27,000	252	370	0.50	1.600
28,000	250	355	0.49	1.590
29,000	248	340	0.47	1.580
30,000	246	320	0.45	1.570
31,000	243	310	0.43	1.560
32,000	241	300	0.42	1.545
33,000	239	280	0.41	1.535
34,000	236	270	0.39	1.525
35,000	234	260	0.38	1.510
36,000	232	245	0.37	1.500
37,000	230	235	0.36	1.490

(Continued)

Digitized by Google

TABLE 1 (Continued)

Temperature, Pressure, Density, and Viscosity of the Atmosphere Over the Marshall Islands During the Spring

Altitude (ft)	Temperature (^oK)	Pressure (mb)	Density ($g/cm^3 \cdot 10^3$)	Viscosity (poises $\cdot 10^4$)
38,000	227	225	0.35	1.475
39,000	225	215	0.33	1.465
40,000	223	205	0.32	1.450
41,000	220	195	0.31	1.440
42,000	218	185	0.30	1.430
43,000	215	175	0.29	1.420
44,000	213	165	0.28	1.405
45,000	211	160	0.27	1.395
46,000	209	150	0.26	1.380
47,000	206	145	0.25	1.370
48,000	204	135	0.24	1.355
49,000	201	130	0.23	1.345
50,000	199	125	0.22	1.335
51,000	196	115	0.21	1.320
52,000	194	110	0.20	1.310
53,000	193	105	0.19	1.295
54,000	192	100	0.18	1.285
55,000	191	95	0.17	1.275
56,000	191	90	0.16	1.275
57,000	192	85	0.155	1.280
58,000	193	80	0.145	1.290
59,000	194	77	0.140	1.295
60,000	195	73	0.135	1.300
61,000	197	70	0.125	1.310
62,000	198	66	0.115	1.320
63,000	199	63	0.110	1.325
64,000	201	60	0.105	1.330
65,000	202	56	0.100	1.340
66,000	203	53	0.094	1.345
67,000	205	50	0.088	1.350
68,000	206	48	0.083	1.360
69,000	207	46	0.078	1.365
70,000	208	43	0.073	1.370
71,000	210	41	0.070	1.380
72,000	211	39	0.066	1.385
73,000	213	37	0.062	1.395
74,000	214	35	0.058	1.400
75,000	215	33	0.054	1.405

(Continued)

Digitized by Google

TABLE 1 (Continued)

Temperature, Pressure, Density, and Viscosity of the Atmosphere Over the Marshall Islands During the Spring

Altitude (ft)	Temperature (°K)	Pressure (mb)	Density ($g/cm^3 \cdot 10^3$)	Viscosity (poises $\cdot 10^4$)
76,000	217	32	0.052	1.415
77,000	218	30	0.049	1.420
78,000	219	28	0.046	1.430
79,000	221	27	0.044	1.435
80,000	222	26	0.042	1.440
81,000	223	24	0.039	1.450
82,000	225	23	0.037	1.455
83,000	226	22	0.034	1.465
84,000	227	21	0.032	1.470
85,000	229	20	0.030	1.480
86,000	230	19	0.029	1.485
87,000	231	18	0.027	1.490
88,000	233	17	0.026	1.500
89,000	234	16	0.024	1.505
90,000	235	15	0.023	1.510
91,000	237	14.5	0.021	1.520
92,000	238	14	0.020	1.525
93,000	239	13	0.019	1.535
94,000	241	12.5	0.018	1.540
95,000	242	12	0.017	1.550
96,000	243	11	0.016	1.555
97,000	245	10.5	0.015	1.565
98,000	246	10	0.014	1.570
99,000	247	9.5	0.013	1.575
100,000	249	9	0.013	1.585
101,000	250	8.5	0.010	1.590
102,000	251	8	0.010	1.600
103,000	253	7.6	0.010	1.605
104,000	254	7.4	0.010	1.610
105,000	255	7.0	0.0095	1.620
106,000	257	6.6	0.0090	1.625
107,000	258	6.2	0.0085	1.635
108,000	259	6.0	0.0080	1.640
109,000	261	5.6	0.0075	1.650
110,000	262	5.4	0.0070	1.655
111,000	263	5.1	0.0068	1.660

(Continued)

Digitized by Google

TABLE 1 (Concluded)

Temperature, Pressure, Density, and Viscosity of the Atmosphere Over the Marshall Islands During the Spring

Altitude (ft)	Temperature (^oK)	Pressure (mb)	Density ($g/cm^3 \cdot 10^3$)	Viscosity ($poises \cdot 10^4$)
112,000	265	4.9	0.0064	1.670
113,000	266	4.6	0.0060	1.675
114,000	267	4.4	0.0056	1.685
115,000	269	4.2	0.0054	1.690
116,000	270	3.9	0.0050	1.700
117,000	271	3.7	0.0048	1.705
118,000	273	3.6	0.0044	1.710
119,000	274	3.4	0.0042	1.720
120,000	275	3.2	0.0040	1.725

Digitized by Google

TABLE 2

Falling Speeds as a Function of Altitude (ft/hr)

Altitude (10^3 ft)	Particle Diameter 75 μ	100 μ	200 μ	350 μ
0	3060	5040	11,700	21,600
5	3120	5240	12,300	22,900
10	3200	5480	12,900	24,100
15	3270	5750	13,700	25,500
20	3360	5980	14,400	27,100
25	3470	6160	15,300	28,800
30	3570	6380	16,300	30,800
35	3720	6640	17,500	33,000
40	3870	6910	18,600	35,300
45	4040	7200	19,800	37,800
50	4210	7520	21,400	40,600
55	4420	7860	23,200	44,600
60	4200	7700	24,400	47,200
65	4190	7480	26,100	51,100
70	4110	7320	27,600	55,200
75	4010	7150	28,100	59,700
80	3910	6960	27,800	61,900
85	3800	6770	27,100	67,800
90	3720	6640	26,500	71,300
95	3620	6470	25,800	77,300
100	3550	6340	25,300	80,200
105	3470	6180	24,800	75,800
110	3400	6050	24,000	74,200
115	3330	5930	23,700	72,600
120	3260	5800	23,400	71,100

Digitized by Google

TABLE 3

Cumulative Time of Fall for the 75-μ Particles (hr)

Intermediate Altitude	Starting Elevation x 10^3 ft 120-115	115-110	110-105	105-100	100-95	95-90	90-85	85-80	80-75	75-70	70-65	65-60
120-115	1.52											
115-110	3.01	1.49										
110-105	4.46	2.94	1.45									
105-100	5.88	4.36	2.87	1.42								
100- 95	7.27	5.75	4.26	2.81	1.39							
95- 90	8.63	7.11	5.62	4.17	2.75	1.36						
90- 85	9.96	8.44	6.95	5.50	4.08	2.69	1.33					
85- 80	11.26	9.74	8.25	6.80	5.38	3.99	2.63	1.30				
80- 75	12.52	11.00	9.51	8.06	6.64	5.25	3.89	2.56	1.26			
75- 70	13.75	12.23	10.74	9.29	7.87	6.48	5.12	3.79	2.49	1.23		
70- 65	14.95	13.43	11.94	10.49	9.07	7.68	6.32	4.99	3.69	2.43	1.20	
65- 60	16.14	14.62	13.13	11.68	10.26	8.87	7.51	6.18	4.88	3.62	2.39	1.19
60- 55	17.30	15.78	14.29	12.84	11.42	10.03	8.67	7.34	6.04	4.78	3.55	2.35
55- 50	18.46	16.94	15.45	14.00	12.58	11.19	9.83	8.50	7.20	5.94	4.71	3.51
50- 45	19.67	18.15	16.66	15.21	13.79	12.40	11.04	9.71	8.41	7.15	5.92	4.72
45- 40	20.93	19.41	17.92	16.47	15.05	13.66	12.30	10.97	9.67	8.41	7.18	5.98
40- 35	22.25	20.73	19.24	17.79	16.37	14.98	13.62	12.29	10.99	9.73	8.50	7.30
35- 30	23.62	22.10	20.61	19.16	17.74	16.35	14.99	13.66	12.36	11.10	9.87	8.67
30- 25	25.04	23.52	22.03	20.58	19.16	17.77	16.41	15.08	13.78	12.52	11.29	10.09
25- 20	26.50	24.98	23.49	22.04	20.62	19.23	17.87	16.54	15.24	13.98	12.75	11.55
20- 15	28.01	26.49	25.00	23.55	22.13	20.74	19.38	18.05	16.75	15.49	14.26	13.06
15- 10	29.55	28.03	26.54	25.09	23.67	22.28	20.92	19.59	18.29	17.03	15.80	14.60
10- 5	31.13	29.61	28.12	26.67	25.25	23.86	22.50	21.17	19.87	18.61	17.38	16.18
5- 0	32.75	31.23	29.74	28.29	26.87	25.48	24.12	22.79	21.49	20.23	19.00	17.80

Digitized by Google

TABLE 3 (Continued)

Cumulative Time of Fall for the 75-μ Particles (hr)

Intermediate Altitude	Starting Elevation x 10^3 ft 60-55	55-50	50-45	45-40	40-35	35-30	30-25	25-20	20-15	15-10	10-5	5-0
120-115												
115-110												
110-105												
105-100												
100- 95												
95- 90												
90- 85												
85- 80												
80- 75												
75- 70												
70- 65												
65- 60												
60- 55	1.16											
55- 50	2.32	1.16										
50- 45	3.53	2.37	1.21									
45- 40	4.79	3.63	2.47	1.26								
40- 35	6.11	4.95	3.79	2.58	1.32							
35- 30	7.48	6.32	5.16	3.95	2.69	1.37						
30- 25	8.90	7.74	6.58	5.37	4.11	2.79	1.42					
25- 20	10.36	9.20	8.04	6.83	5.57	4.25	2.88	1.46				
20- 15	11.87	10.71	9.55	8.34	7.08	5.76	4.39	2.97	1.51			
15- 10	13.41	12.25	11.09	9.88	8.62	7.30	5.93	4.51	3.05	1.54		
10- 5	14.99	13.83	12.67	11.46	10.20	8.88	7.51	6.09	4.63	3.12	1.58	
5- 0	16.61	15.45	14.29	13.08	11.82	10.52	9.13	7.71	6.25	4.74	3.20	1.62

Digitized by Google

TABLE 4

Cumulative Time of Fall for the 100-μ Particles (hr)

Intermediate Altitude	Starting Elevation x 10^3 ft: 120-115	115-110	110-105	105-100	100-95	95-90	90-85	85-80	80-75	75-70	70-65	65-60
120-115	0.85											
115-110	1.68	0.83										
110-105	2.50	1.65	0.82									
105-100	3.30	2.45	1.62	0.80								
100- 95	4.08	3.23	2.40	1.58	0.78							
95- 90	4.84	3.99	3.16	2.34	1.54	0.76						
90- 85	5.58	4.73	3.90	3.08	2.28	1.50	0.74					
85- 80	6.30	5.46	4.63	3.81	3.01	2.23	1.47	0.73				
80- 75	7.02	6.17	5.34	4.52	3.72	2.94	2.18	1.44	0.71			
75- 70	7.71	6.86	6.03	5.21	4.41	3.63	2.87	2.13	1.40	0.69		
70- 65	8.38	7.53	6.70	5.88	5.08	4.30	3.54	2.80	2.07	1.36	0.67	
65- 60	9.04	8.19	7.36	6.54	5.74	4.96	4.20	3.46	2.73	2.02	1.33	0.66
60- 55	9.68	8.83	8.00	7.18	6.38	5.60	4.84	4.10	3.37	2.66	1.97	1.30
55- 50	10.33	9.48	8.65	7.83	7.03	6.25	5.49	4.75	4.02	3.31	2.62	1.95
50- 45	11.01	10.16	9.33	8.51	7.71	6.93	6.17	5.43	4.70	3.99	3.30	2.63
45- 40	11.72	10.87	10.04	9.22	8.42	7.64	6.88	6.14	5.41	4.70	4.01	3.34
40- 35	12.46	11.61	10.78	9.96	9.16	8.38	7.62	6.88	6.15	5.44	4.75	4.08
35- 30	13.24	12.39	11.56	10.74	9.94	9.16	8.40	7.66	6.93	6.22	5.53	4.86
30- 25	14.03	13.18	12.35	11.53	10.73	9.95	9.19	8.45	7.72	7.01	6.32	5.65
25- 20	14.85	14.00	13.17	12.35	11.55	10.77	10.01	9.27	8.54	7.83	7.14	6.47
20- 15	15.70	14.85	14.02	13.20	12.40	11.62	10.86	10.12	9.39	8.68	7.99	7.32
15- 10	16.59	15.74	14.91	14.09	13.29	12.51	11.75	11.01	10.28	9.57	8.88	8.21
10- 5	17.52	16.67	15.84	15.02	14.22	13.44	12.68	11.94	11.21	10.50	9.81	9.14
5- 0	18.49	17.64	16.81	15.99	15.19	14.41	13.65	12.91	12.18	11.47	10.78	10.11

Digitized by Google

TABLE 4 (Continued)

Cumulative Time of Fall for the 100-μ Particles (hr)

Intermediate Altitude	Starting Elevation x 10^3 ft											
	60-55	55-50	50-45	45-40	40-35	35-30	30-25	25-20	20-15	15-10	10-5	5-0
120-115												
115-110												
110-105												
105-100												
100- 95												
95- 90												
90- 85												
85- 80												
80- 75												
75- 70												
70- 65												
65- 60												
60- 55	0.64											
55- 50	1.29	0.65										
50- 45	1.97	1.33	0.68									
45- 40	2.68	2.04	1.39	0.71								
40- 35	3.42	2.78	2.13	1.45	0.74							
35- 30	4.20	3.56	2.91	2.23	1.52	0.78						
30- 25	4.99	4.35	3.70	3.02	2.31	1.57	0.79					
25- 20	5.81	5.17	4.52	3.84	3.13	2.39	1.61	0.82				
20- 15	6.66	6.02	5.37	4.69	3.98	3.24	2.46	1.67	0.85			
15- 10	7.55	6.91	6.26	5.58	4.87	4.13	3.35	2.56	1.74	0.89		
10- 5	8.48	7.84	7.19	6.51	5.80	5.06	4.28	3.49	2.67	1.82	0.93	
5- 0	9.45	8.81	8.16	7.48	6.77	6.03	5.25	4.46	3.64	2.79	1.90	0.97

Digitized by Google

TABLE 5
Cumulative Time of Fall for 200-μ Particles (hr)

Intermediate Altitude	Starting Elevation x 10^3 ft											
	120-115	115-110	110-105	105-100	100-95	95-90	90-85	85-80	80-75	75-70	70-65	65-60
120-115	0.21											
115-110	0.42	0.21										
110-105	0.62	0.41	0.20									
105-100	0.82	0.61	0.40	0.20								
100- 95	1.02	0.81	0.60	0.40	0.20							
95- 90	1.21	1.00	0.79	0.59	0.39	0.19						
90- 85	1.40	1.19	0.98	0.78	0.58	0.38	0.19					
85- 80	1.58	1.37	1.16	0.96	0.76	0.56	0.37	0.18				
80- 75	1.76	1.55	1.34	1.14	0.94	0.74	0.55	0.36	0.18			
75- 70	1.94	1.73	1.52	1.32	1.12	0.92	0.73	0.54	0.36	0.18		
70- 65	2.13	1.92	1.71	1.51	1.31	1.11	0.92	0.73	0.55	0.37	0.19	
65- 60	2.33	2.12	1.91	1.71	1.51	1.31	1.12	0.93	0.75	0.57	0.39	0.20
60- 55	2.54	2.33	2.12	1.92	1.72	1.52	1.33	1.14	0.96	0.78	0.60	0.41
55- 50	2.76	2.55	2.34	2.14	1.94	1.74	1.55	1.36	1.18	1.00	0.82	0.63
50- 45	3.00	2.79	2.58	2.38	2.18	1.98	1.79	1.60	1.42	1.24	1.06	0.87
45- 40	3.26	3.05	2.84	2.64	2.44	2.24	2.05	1.86	1.68	1.50	1.32	1.13
40- 35	3.54	3.33	3.12	2.92	2.72	2.52	2.33	2.14	1.96	1.78	1.60	1.41
35- 30	3.84	3.63	3.42	3.22	3.02	2.82	2.63	2.44	2.26	2.08	1.90	1.71
30- 25	4.16	3.95	3.74	3.54	3.34	3.14	2.95	2.76	2.58	2.40	2.22	2.03
25- 20	4.50	4.29	4.08	3.88	3.68	3.48	3.29	3.10	2.92	2.74	2.56	2.37
20- 15	4.86	4.65	4.44	4.24	4.04	3.84	3.65	3.46	3.28	3.10	2.92	2.73
15- 10	5.24	5.03	4.82	4.62	4.42	4.22	4.03	3.84	3.66	3.48	3.30	3.11
10- 5	5.64	5.43	5.22	5.02	4.82	4.62	4.43	4.24	4.06	3.88	3.70	3.51
5- 0	6.06	5.85	5.64	5.44	5.24	5.04	4.85	4.66	4.48	4.30	4.12	3.93

Digitized by Google

TABLE 5 (Continued)

Cumulative Time of Fall for 200-μ Particles (hr)

Intermediate Altitude	Starting Elevation x 10^3 ft 60-55	55-50	50-45	45-40	40-35	35-30	30-25	25-20	20-15	15-10	10-5	5-0
120-115												
115-110												
110-105												
105-100												
100- 95												
95- 90												
90- 85												
85- 80												
80- 75												
75- 70												
70- 65												
65- 60												
60- 55	0.21											
55- 50	0.43	0.22										
50- 45	0.67	0.46	0.24									
45- 40	0.93	0.72	0.50	0.26								
40- 35	1.21	1.00	0.78	0.54	0.28							
35- 30	1.51	1.30	1.08	0.84	0.58	0.30						
30- 25	1.83	1.62	1.40	1.16	0.90	0.62	0.32					
25- 20	2.17	1.96	1.74	1.50	1.24	0.96	0.66	0.34				
20- 15	2.53	2.32	2.10	1.86	1.60	1.32	1.02	0.70	0.36			
15- 10	2.91	2.70	2.48	2.24	1.98	1.70	1.40	1.08	0.74	0.38		
10- 5	3.31	3.10	2.88	2.64	2.38	2.10	1.80	1.48	1.14	0.78	0.40	
5- 0	3.73	3.52	3.30	3.06	2.80	2.52	2.22	1.90	1.56	1.20	0.82	0.42

Digitized by Google

TABLE 6

Cumulative Time of Fall for 350-μ Particles (hr)

Intermediate Altitude	Starting Elevation x 10^3 ft 120-115	115-110	110-105	105-100	100-95	95-90	90-85	85-80	80-75	75-70	70-65	65-60
120-115	0.07											
115-110	0.14	0.07										
110-105	0.21	0.14	0.07									
105-100	0.27	0.20	0.13	0.06								
100- 95	0.33	0.26	0.19	0.12	0.06							
95- 90	0.40	0.33	0.26	0.19	0.13	0.07						
90- 85	0.47	0.40	0.33	0.26	0.20	0.14	0.07					
85- 80	0.55	0.48	0.41	0.34	0.28	0.22	0.15	0.08				
80- 75	0.63	0.56	0.49	0.42	0.36	0.30	0.23	0.16	0.08			
75- 70	0.72	0.65	0.58	0.51	0.45	0.39	0.32	0.25	0.17	0.09		
70- 65	0.81	0.74	0.67	0.60	0.54	0.48	0.41	0.34	0.26	0.18	0.09	
65- 60	0.91	0.84	0.77	0.70	0.64	0.58	0.51	0.44	0.36	0.28	0.19	0.10
60- 55	1.02	0.95	0.88	0.81	0.75	0.69	0.62	0.55	0.47	0.39	0.30	0.21
55- 50	1.14	1.07	1.00	0.93	0.87	0.81	0.74	0.67	0.59	0.51	0.42	0.33
50- 45	1.27	1.20	1.13	1.06	1.00	0.94	0.87	0.80	0.72	0.64	0.55	0.46
45- 40	1.41	1.34	1.27	1.20	1.14	1.08	1.01	0.94	0.86	0.78	0.69	0.60
40- 35	1.56	1.49	1.42	1.35	1.29	1.23	1.16	1.09	1.01	0.93	0.84	0.75
35- 30	1.72	1.65	1.58	1.51	1.45	1.39	1.32	1.25	1.17	1.09	1.00	0.91
30- 25	1.89	1.82	1.75	1.68	1.62	1.56	1.49	1.42	1.34	1.26	1.17	1.08
25- 20	2.07	2.00	1.93	1.86	1.80	1.74	1.67	1.60	1.52	1.44	1.35	1.26
20- 15	2.26	2.19	2.12	2.05	1.99	1.93	1.86	1.79	1.71	1.63	1.54	1.45
25- 10	2.46	2.39	2.32	2.25	2.19	2.13	2.06	1.99	1.91	1.83	1.74	1.65
10- 5	2.67	2.60	2.53	2.46	2.40	2.34	2.27	2.20	2.12	2.04	1.95	1.86
5- 0	2.89	2.82	2.75	2.68	2.62	2.56	2.49	2.42	2.34	2.26	2.17	2.08

Digitized by Google

TABLE 6 (Continued)

Cumulative Time of Fall for 350-μ Particles (hr)

Intermediate Altitude	Starting Elevation x 10^3 ft 60-55	55-50	50-45	45-40	40-35	35-30	30-25	25-20	20-15	15-10	10-5	5-0
120-115												
115-110												
110-105												
105-100												
100- 95												
95- 90												
90- 85												
85- 80												
80- 75												
75- 70												
70- 65												
65- 60												
60- 55	0.11											
55- 50	0.23	0.12										
50- 45	0.36	0.25	0.13									
45- 40	0.50	0.39	0.27	0.14								
40- 35	0.65	0.54	0.42	0.29	0.15							
35- 30	0.81	0.70	0.58	0.45	0.31	0.16						
30- 25	0.98	0.87	0.75	0.62	0.48	0.33	0.17					
25- 20	1.16	1.05	0.93	0.80	0.66	0.51	0.35	0.18				
20- 15	1.35	1.24	1.12	0.99	0.85	0.70	0.54	0.37	0.19			
15- 10	1.55	1.44	1.32	1.19	1.05	0.90	0.74	0.57	0.39	0.20		
10- 5	1.76	1.65	1.53	1.40	1.26	1.11	0.95	0.78	0.60	0.41	0.21	
5- 0	1.98	1.87	1.75	1.62	1.48	1.33	1.17	1.00	0.82	0.63	0.43	0.22

Digitized by Google

DISTRIBUTION

COPIES	
	NAVY
1-9	Chief, Bureau of Ships (Code 233)
10	Chief, Bureau of Medicine and Surgery
11	Chief, Bureau of Aeronautics (Code AE40)
12	Chief, Bureau of Supplies and Accounts (Code W)
13-14	Chief, Bureau of Yards and Docks (D-440)
15	Chief of Naval Research (Code 811)
16	Chief of Naval Operations (Op-36)
17	Commander, New York Naval Shipyard (Material Lab.)
18-20	Director, Naval Research Laboratory (Code 2021)
21-22	CO, Office of Naval Research, New York
23	Naval Medical Research Institute
24	CO, Naval Unit, Army Chemical Center
25	CO, Naval Unit, CmlC Training Command
26	CO, U.S. Naval Civil Engineering (Res. and Eval. Lab.)
27	U.S. Naval School (CEC Officers)
28	Commander, Naval Air Material Center, Philadelphia
29	CO, Naval Schools Command, Treasure Island
30	CO, Naval Damage Control Training Center, Philadelphia
31	U.S. Naval Postgraduate School, Monterey
32	CO, Fleet Training Center, Norfolk
33-34	CO, Fleet Training Center, San Diego
35	Commandant, Twelfth Naval District
36	Office of Patent Counsel, Mare Island
37	Office of Naval Research Branch Office, S.F.
38	Commander Air Force, Atlantic Fleet (Code 16F)
39	CO, Fleet Airborne Electronics Training Unit Atlantic
40	Commandant, U.S. Marine Corps
41	Commandant, Marine Corps Schools, Quantico (Library)
42	Commandant, Marine Corps Schools, Quantico (Dev. Center)
	ARMY
43	Chief of Engineers (ENGEB, Dhein)
44	Chief of Engineers (ENGNB)
45-46	Chief of Research and Development (Atomic Division)

Digitized by Google

47 Chief of Transportation (TC Technical Committee)
48 Chief of Ordnance (ORDTB)
49 Chief Chemical Officer
50 Deputy Chief of Staff for Military Operations
51 CG, Chemical Research and Development Command
52 CO, Chemical Corps Materiel Command
53-54 Chemical and Radiological Laboratories, ACmlC
55 CO, Chemical Corps Medical Laboratories
56 President, Chemical Corps Board
57-58 Ordnance Department, Aberdeen Proving Ground
59 CO, Chemical Corps Training Command (Library)
60 CO, Chemical Field Requirements Agency
61-62 CO, Chemical Warfare Laboratories
63 Office of Chief Signal Officer (SIGRD-8B)
64 CO, Army Medical Research Laboratory
65 Director, Walter Reed Army Medical Center
66 CG, Continental Army Command, Fort Monroe (ATDEV-1)
67 Army Medical Service Graduate School (Dept. of Biophysics)
68 CG, Quartermaster Res. and Dev. Command
69 Director, Operations Research Office (Librarian)
70 CO,Dugway Proving Ground
71 Director, Evans Signal Laboratory (Nucleonics Section)
72 CG, Engineer Res. and Dev. Laboratory (Library)
73 CO, Transportation Res. and Dev. Command, Fort Eustis
74 Commandant, Army Aviation School, Fort Rucker
75 President, Board No. 6, CONARC, Fort Rucker
76 CO, CONARC, Ft. Monroe
77 Director, Office of Special Weapons Development
78 CG, Redstone Arsenal
79 CO, Ordnance Materials Research Office, Watertown
80 CO, Watertown Arsenal
81 CO, Frankford Arsenal
82 Signal Corps Center, Fort Monmouth
83 Director, Jet Propulsion Laboratory
84 Tokyo Army Hospital

AIR FORCE

85 Commander, Air Materiel Command (MCMTM)
86 Commander, Wright Air Development Center (WCRTY)
87 Commander, Wright Air Development Center (WCRTH-1)
88 Commander, Air Res. and Dev. Command (RDTDA)
89 Director, USAF Project RAND (WEAPD)
90 Commandant, School of Aviation Medicine
91 USAF, SAM, Randolph Field (Brooks)
92 CG, Strategic Air Command, Offutt Air Force Base (IGABD)
93 CG, Strategic Air Command (Operations Analysis Office)

Digitized by Google

94	Commander, Kirtland Air Force Base
95	Office of Surgeon General
96	Director, Air University Library, Maxwell Air Force Base
97-98	Commander, Technical Training Wing, 3415th TTG
99	CG, Cambridge Research Center (CRHTM)

OTHER DOD ACTIVITIES

100	Chief, Armed Forces Special Weapons Project
101	AFSWP, SWTG, Sandia Base (Library)
102-104	AFSWP, Hq., Field Command, Sandia Base
105	Assistant Secretary of Defense (Res. and Dev.)
106-107	Assistant Secretary of Defense (Civil Defense Division)
108-112	Armed Services Technical Information Agency

AEC ACTIVITIES AND OTHERS

113	Alco Products, Inc.
114	Argonne Cancer Research Hospital
115-120	Argonne National Laboratory
121	Atomic Bomb Casualty Commission
122-124	Atomic Energy Commission, Washington
125-126	Atomics International
127-128	Battelle Memorial Institute
129-132	Bettis Plant
133	Boeing Airplane Company
134-137	Brookhaven National Laboratory
138	Brush Beryllium Company
139	Carnegie Institute of Technology
140	Chicago Patent Group
141	Columbia University (Hassialis)
142-143	Columbia University (Havens)
144	Combustion Engineering, Inc.
145-146	Consolidated Vultee Aircraft Corporation
147-148	Convair-General Dynamics Corporation (Helms)
149-150	Division of Raw Materials, Denver
151	Dow Chemical Company, Rocky Flats
152-155	duPont Company, Aiken
156	duPont Company, Wilmington
157-158	General Electric Company (ANPP)
159-162	General Electric Company, Richland
163-165	Goodyear Atomic Corporation
166-167	Iowa State College
168-170	Knolls Atomic Power Laboratory
171-172	Lockheed Aircraft Corporation (Cleveland)
173	Lockheed Aircraft Corporation, Marietta

Digitized by Google

174-175	Los Alamos Scientific Laboratory
176	Massachusetts Institute of Technology (Hardy)
177	Mound Laboratory
178	National Advisory Committee for Aeronautics
179	National Bureau of Standards (Library)
180-181	National Bureau of Standards (Taylor)
182	National Lead Company of Ohio
183	New Brunswick Laboratory
184	New York Operations Office
185	New York University
186	Nuclear Development Corporation of America
187	Nuclear Metals, Inc. (Kaufmann)
188	Oak Ridge Institute of Nuclear Studies
189-194	Oak Ridge National Laboratory
195	Patent Branch, Washington
196	Patent Office, Department of Commerce
197	Pennsylvania State University (Blanchard)
198-203	Phillips Petroleum Company
204	Princeton University (White)
205-206	Public Health Service, Washington
207	RAND Corporation
208	Sandia Corporation
209	Technical Operations Inc. (Hudson)
210	Union Carbide Nuclear Company (C-31 Plant)
211-212	Union Carbide Nuclear Company (K-25 Plant)
213	United Aircraft Corporation
214	U.S. Geological Survey, Denver
215	U.S. Geological Survey, Menlo Park
216	U.S. Geological Survey, Naval Gun Factory
217	U.S. Geological Survey, Washington
218	UCLA Medical Research Laboratory
219-220	University of California Radiation Laboratory, Berkeley
221-224	University of California Radiation Laboratory, Livermore
225	University of Rochester (Technical Report Unit)
226-227	University of Rochester (Marshak)
228	University of Utah (Stoner)
229	University of Washington (Manley)
230	Vitro Engineering Division
231	Weil, Dr. George L.
232-233	Western Reserve University
234	Yale University (Breit)
235	Yale University (Wadey)
236-260	Technical Information Service Extension, Oak Ridge

USNRDL

261-300	USNRDL, Technical Information Division

DATE ISSUED: 25 April 1957

Digitized by Google

Naval Radiological Defense Laboratory.
USNRDL-TR-139.
A FALLOUT FORECASTING TECHNIQUE WITH RESULTS OBTAINED AT THE ENIWETOK PROVING GROUND, by E.A. Schuert. 3 Apr. 1957. 60 p. illus. UNCLASSIFIED

A generalized fallout forecasting technique is presented with detailed computations of input parameters which were used at the Eniwetok Proving Ground.

Results obtained at a recent weapons test are
(over)

1. Fallout
2. Radioactive substances
3. Particles (Airborne)

I. Schuert, E.A.
II. Title
III. Operation REDWING
IV. NS 081-001.

UNCLASSIFIED

Naval Radiological Defense Laboratory.
USNRDL-TR-139.
A FALLOUT FORECASTING TECHNIQUE WITH RESULTS OBTAINED AT THE ENIWETOK PROVING GROUND, by E.A. Schuert. 3 Apr. 1957. 60 p. illus. UNCLASSIFIED

A generalized fallout forecasting technique is presented with detailed computations of input parameters which were used at the Eniwetok Proving Ground.

Results obtained at a recent weapons test are
(over)

1. Fallout
2. Radioactive substances
3. Particles (Airborne)

I. Schuert, E.A.
II. Title
III. Operation REDWING
IV. NS 081-001.

UNCLASSIFIED

Naval Radiological Defense Laboratory.
USNRDL-TR-139.
A FALLOUT FORECASTING TECHNIQUE WITH RESULTS OBTAINED AT THE ENIWETOK PROVING GROUND, by E.A. Schuert. 3 Apr. 1957. 60 p. illus. UNCLASSIFIED

A generalized fallout forecasting technique is presented with detailed computations of input parameters which were used at the Eniwetok Proving Ground.

Results obtained at a recent weapons test are
(over)

1. Fallout
2. Radioactive substances
3. Particles (Airborne)

I. Schuert, E.A.
II. Title
III. Operation REDWING
IV. NS 081-001.

UNCLASSIFIED

Naval Radiological Defense Laboratory.
USNRDL-TR-139.
A FALLOUT FORECASTING TECHNIQUE WITH RESULTS OBTAINED AT THE ENIWETOK PROVING GROUND, by E.A. Schuert. 3 Apr. 1957. 60 p. illus. UNCLASSIFIED

A generalized fallout forecasting technique is presented with detailed computations of input parameters which were used at the Eniwetok Proving Ground.

Results obtained at a recent weapons test are
(over)

1. Fallout
2. Radioactive substances
3. Particles (Airborne)

I. Schuert, E.A.
II. Title
III. Operation REDWING
IV. NS 081-001.

UNCLASSIFIED

Digitized by Google

briefly discussed by comparison of forecast fallout with preliminary measured data.

UNCLASSIFIED

briefly discussed by comparison of forecast fallout with preliminary measured data.

UNCLASSIFIED

UNCLASSIFIED

briefly discussed by comparison of forecast fallout with preliminary measured data.

UNCLASSIFIED

UNCLASSIFIED

briefly discussed by comparison of forecast fallout with preliminary measured data.

UNCLASSIFIED

Digitized by Google

Naval Radiological Defense Laboratory.
USNRDL-TR-139.
A FALLOUT FORECASTING TECHNIQUE WITH RESULTS OBTAINED AT THE ENIWETOK PROVING GROUND, by E.A. Schuert. 3 Apr. 1957. 60 p. illus. UNCLASSIFIED

A generalized fallout forecasting technique is presented with detailed computations of input parameters which were used at the Eniwetok Proving Ground.

Results obtained at a recent weapons test are
(over)

1. Fallout
2. Radioactive substances
3. Particles (Airborne)

I. Schuert, E.A.
II. Title
III. Operation REDWING
IV. NS 081-001.

UNCLASSIFIED

Naval Radiological Defense Laboratory.
USNRDL-TR-139.
A FALLOUT FORECASTING TECHNIQUE WITH RESULTS OBTAINED AT THE ENIWETOK PROVING GROUND, by E.A. Schuert. 3 Apr. 1957. 60 p. illus. UNCLASSIFIED

A generalized fallout forecasting technique is presented with detailed computations of input parameters which were used at the Eniwetok Proving Ground.

Results obtained at a recent weapons test are
(over)

1. Fallout
2. Radioactive substances
3. Particles (Airborne)

I. Schuert, E.A.
II. Title
III. Operation REDWING
IV. NS 081-001.

UNCLASSIFIED

Naval Radiological Defense Laboratory.
USNRDL-TR-139.
A FALLOUT FORECASTING TECHNIQUE WITH RESULTS OBTAINED AT THE ENIWETOK PROVING GROUND, by E.A. Schuert. 3 Apr. 1957. 60 p. illus. UNCLASSIFIED

A generalized fallout forecasting technique is presented with detailed computations of input parameters which were used at the Eniwetok Proving Ground.

Results obtained at a recent weapons test are
(over)

1. Fallout
2. Radioactive substances
3. Particles (Airborne)

I. Schuert, E.A.
II. Title
III. Operation REDWING
IV. NS 081-001.

UNCLASSIFIED

Naval Radiological Defense Laboratory.
USNRDL-TR-139.
A FALLOUT FORECASTING TECHNIQUE WITH RESULTS OBTAINED AT THE ENIWETOK PROVING GROUND, by E.A. Schuert. 3 Apr. 1957. 60 p. illus. UNCLASSIFIED

A generalized fallout forecasting technique is presented with detailed computations of input parameters which were used at the Eniwetok Proving Ground.

Results obtained at a recent weapons test are
(over)

1. Fallout
2. Radioactive substances
3. Particles (Airborne)

I. Schuert, E.A.
II. Title
III. Operation REDWING
IV. NS 081-001.

UNCLASSIFIED

Digitized by Google

<u>UNCLASSIFIED</u>

briefly discussed by comparison of forecast fallout with preliminary measured data.

<u>UNCLASSIFIED</u>

<u>UNCLASSIFIED</u>

briefly discussed by comparison of forecast fallout with preliminary measured data.

<u>UNCLASSIFIED</u>

<u>UNCLASSIFIED</u>

briefly discussed by comparison of forecast fallout with preliminary measured data.

<u>UNCLASSIFIED</u>

<u>UNCLASSIFIED</u>

briefly discussed by comparison of forecast fallout with preliminary measured data.

<u>UNCLASSIFIED</u>

Digitized by Google

Digitized by Google

Digitized by Google